Downloaded from orbit.dtu.dk on: May 04, 2023

DTU Library

# Lowering district heating temperatures – Impact to system performance in current and future Danish energy scenarios

**Ommen, Torben; Markussen, Wiebke Brix; Elmegaard, Brian**

*Published in:*
Energy

*Link to article, DOI:*
10.1016/j.energy.2015.10.063

*Publication date:*
2016

*Document Version*
Peer reviewed version

Link back to DTU Orbit

*Citation (APA):*
Ommen, T., Markussen, W. B., & Elmegaard, B. (2016). Lowering district heating temperatures – Impact to system performance in current and future Danish energy scenarios. *Energy*, *94*, 273-291. https://doi.org/10.1016/j.energy.2015.10.063

**General rights**
Copyright and moral rights for the publications made accessible in the public portal are retained by the authors and/or other copyright owners and it is a condition of accessing publications that users recognise and abide by the legal requirements associated with these rights.

- Users may download and print one copy of any publication from the public portal for the purpose of private study or research.
- You may not further distribute the material or use it for any profit-making activity or commercial gain
- You may freely distribute the URL identifying the publication in the public portal

If you believe that this document breaches copyright please contact us providing details, and we will remove access to the work immediately and investigate your claim.

# Lowering district heating temperatures - Impact to system performance in current and future Danish energy scenarios

Torben Ommen[a,*], Wiebke Brix Markussen[a], Brian Elmegaard[a]

[a] *Technical University of Denmark, Kgs. Lyngby, Denmark*

**Abstract**

Combined heat and power (CHP) production in connection with district heating (DH) systems has previously demonstrated a significant reduction in primary energy consumption. With extended installation of intermittent sustainable sources, such as eg. wind turbines rather than thermal units, the changed distribution of generation technologies may suggest a reconsideration of optimum for DH network temperatures, in order to achieve low cost and minimize carbon emissions. A mixed integer linear optimisation model was used to investigate the changed operation based on changed network characteristics. Utility plants and demand curves corresponded to the current and future scenarios for the DH system of Greater Copenhagen. Performance curves from typical CHP-plant technologies were used to represent the changed operation of power and heat production for changed DH temperatures. The results show that primary fuel consumption is reduced approximately 5-7 % at DH design temperatures of 60 - 70 °C. Further reduction in DH temperatures resulted in opposing tendencies, as hot tap water requires electricity to reach the required temperatures. The results are network-specific, as they represent the given network and production units, but similar trends can be expected for other large networks.

*Keywords:* Heat pumps, District heating, Combined heat and power, Optimisation.

## 1 Introduction

Combined heat and power (CHP) production in connection with district heating (DH) systems has resulted in significant reduction in primary energy consumption in Denmark [1]. With power production investments moving from thermal units to intermittent renewable sources, such as eg. wind turbines or solar photovoltaics technology [2], the excess heat co-generated with power is decreased.
The changed distribution between thermal and intermittent technologies for electricity suggest changes to the corresponding technologies for supplying heat to the DH network. As investment in new utility technologies is required, it is suggested also to consider the influence of DH network temperatures for a complete system optimization. The choice of temperatures does not only affect network heat losses, but also impacts network capacities, and changes the possible benefit of different technologies. Thus it is likely that two different choices in network temperatures will result in two significantly different optimal technology distributions, and vice versa.
In Denmark, the investment in future utility production units is constrained to renewable technologies due to political zero carbon emission ambitions (eg. Danish Government [3]). Such ambitions are also represented in the local communities. The city council of Copenhagen agreed in 2013 on a climate plan attempting to make Copenhagen the first $CO_2$ neutral capital in 2025 [4]. Carbon neutral heating and power production is naturally key focuses to achieve such goals. As the DH network supplies 98% of the heat demand in the

*Corresponding author

*Email addresses:* tsom@mek.dtu.dk (Torben Ommen), wb@mek.dtu.dk (Wiebke Brix Markussen), be@mek.dtu.dk (Brian Elmegaard)

## Nomenclature

| | |
|---|---|
| $\dot{C}$ | cost rate, €/h |
| $C$ | constant |
| $k$ | opening degree, - |
| $\dot{m}$ | massflow, kg/s |
| $p$ | pressure, Pa |
| $T$ | temperature, °C |
| | |
| Greek symbols | |
| $\alpha$ | flow characteristic |
| $\beta$ | power loss factor for heat extraction |
| $\Delta$ | variation or glide |
| $\rho$ | density, kg/m$^3$ |
| | |
| Subscripts | |
| $C$ | consumer |
| cond | condensation |
| $E$ | exiting consumer |
| evap | evaporation |
| elec | electric |
| $F$ | forward |
| $f$, $g$, $h$, $i$, $j$ | index |
| in | inlet |
| out | outlet |
| $R$ | return |
| sink | sink reservoir |
| source | source reservoir |
| $T$ | turbine |
| $t$ | hours |
| total | total utilisation |
| | |
| Abbreviations | |
| CC | Combined Cycle |
| CHP | Combined Heat and Power |
| COP | Coefficient Of Performance |
| DH | District Heating |
| Gen | Generator |
| HP(s) | Heat Pump(s) |

Copenhagen municipality, these utility production units are of main concern. The climate plan proposes to convert central CHP units to biomass and integrating central, large-scale heat pumps (HPs) in the DH networks as two feasible measures.

A series of previously published reports named "Heat Plan Greater Copenhagen" (in Danish "Varmeplan Hovedstaden"), of which the newest at the time of writing is number 3, concludes that a limited share (300 MW installed capacity) of central heat pumps, may provide small reductions in heat cost after 2030-35 [5]. According to their calculations, the use of sustainable biomass is the major driver for cost and carbon reductions in the future system. With one highly dominant fuel type, the system may, however, experience a significant reduction in security of supply.

Four explanations are conceivable for the expected poor penetration of heat pumps in the future technology composition for DH:

1 The extraction CHP plant technology provides highly efficient conversion of electricity to heat (typically approx. ratio: 7-11:1 [6]) according to the power loss factors by heat extraction [7]. This is a performance advantage in the order of a factor of 3 compared to the HP technology [8].

2 Low coefficient of performance (COP) from integrating HPs to supply heat in the transmission network at 90 °C or above [9]. With low COP the HP utilises large quantities of electricity, which in addition to the cost of electricity also carries significant network losses and taxes. Heat can be co-supplied at lower temperatures to increase COP (e.g. to the return stream of the network) but such integration schemes increase the operational constraints of the system, and the HPs can in this case not be utilised as a stand alone technology.

3 Taxation for HPs reaches above 50 % of the levelized cost for heat [10] considering the Danish taxation scheme [11].

4 Insufficient heat sources with high temperature, which are located within or close to the DH network perimeter [5, 12]. In case the heat sources are not co-located with the large DH-streams, the investments for HPs are increased significantly.

Item 2 and 3 are addressed by lowering DH temperatures, in this way increasing the COP of the HP unit. As taxation is based on the consumption of electricity for heat production, increasing COP will lower the quantity of the heat cost that originate from taxes.

When the temperature in the DH network is changed, all of the existing types of utility technologies will experience performance changes. In order to fully evaluate the improved performance of the HPs at changed DH temperatures, the performance estimates for existing technologies should also correspond to the changed temperatures.

In this paper, the effects of changing DH temperatures are evaluated in terms of the total cost for heat and electricity for the consumers, carbon emissions and primary fuel consumption. Performance curves from typical CHP-plant technologies are used to represent the changed operation of power and heat production. As large changes are expected for the current network within a limited time-frame, two cases are considered in order to evaluate the implications of changing DH temperatures for the current and future network and utility units. The current energy scenario is assessed by utilising a validated layout for 2011 where steam-based DH networks are utilised in central areas of the network [13]. The future scenario (2025) corresponds closely to that considered in "Heat Plan Greater Copenhagen 2" [14]. Neither of the two scenarios utilises central HPs in DH networks. In the paper two corresponding scenarios are included considering a significant integration (200 MW capacity) of HPs.

To assess the changes to the network capacity corresponding to the current and future design, a DH network model is included, where the changed capacity at changed temperature levels is considered. This allows an analysis of the possibilities for changing network temperatures without further investment in the large transmission and distribution lines of Greater Copenhagen.

The developed model thus represents an existing system as a case, but it is intended to be an illustration of current and future energy systems in cities with high penetration of CHP-based district heating and thus high-efficient heat supply. The study shows the possibilities for optimal integration of intermittent renewables when accounting for the performance of different technologies under different operating temperature conditions.

## 2 Method

Thermodynamic models of representative technologies were used in order to analyse the change in performance of the individual units with changes in temperature of the DH network. The models were programmed in Engineering Equation Solver [15]. These models are further described in section 2.1, 2.2 and 2.3.

A detailed mixed integer linear optimisation model was used to investigate the new operation based on the changed parameters. The model was programmed in Matlab and GAMS using the CPLEX solver [16, 17, 18]. The model was designed and used for the case study of the production technologies and network characteristics of Greater Copenhagen [13], but the implementation of energy system equipment in the model is generic and easy to change to other systems. The heat and power system model is further described in section 2.5 and appendix A.

### *2.1 Temperature of current and future DH networks, network capacities and DH heat losses*

Generally, the temperatures for a district heating network are kept as low as possible in order to reduce heat losses and increase efficiency of electricity co-production. The lower limit for traditional DH forward temperatures is reached when the required temperature of certain constituents of the demand (often approximately 55 °C due to hot tap water) is no longer met.

In a Danish context the forward temperature ($T_{\mathrm{DH,forward}}$) varies from 70 °C to 120 °C [19, 20]. The corresponding network return temperatures ($T_{\mathrm{DH,return}}$) range from 35 °C to 55 °C. The design temperatures of the current DH network and utility units are 100 °C, with temperature variations of 95-110 °C to account for network capacity constraints in cold periods and energy savings in the summer.

In Lund et al. [21] further reduction in temperatures is proposed, with a lower limit of DH design temperatures reaching as low as 40 °C, which is the limit allowed by modern space heating technology (4GDH). In this case electric heaters or booster HP units are required for production of hot tap water [22, 23, 24]. The performance of booster HP units is further addressed in section 2.4. In table 1 both current and future proposals for temperature in DH networks are presented.

Based on the considered temperature sets, the return and forward temperatures were interpolated linearly for the range of $T_{\mathrm{DH,forward}}$ = 40-110 °C and $T_{\mathrm{DH,return}}$ = 20-55 °C as shown in Fig 1.

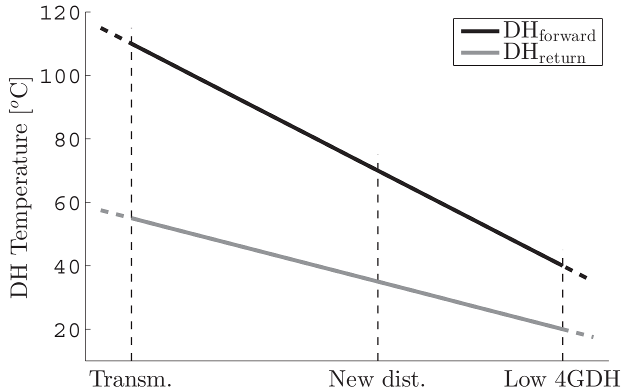


Figure 1: Temperature spans applied of the modelled DH networks.

The temperature levels do not only influence the production technologies, but also the volume flow of DH fluid is significantly changed for a constant amount of transferred heat. As the pressure losses become significant for increasing flow rates in the network [25, 26, 27], the various transmission lines were constrained to a maximal volume flow. The maximal flow rates for the two scenarios were based on a data from a corresponding network model for 2012 and 2025 [5, 12]. Only transmission lines and capacity constraints for large distribution lines were included in the model. The capacity of the individual transmission lines was varied according to the changed temperatures in the model.

Similar constraints were found for sensible heat storages, where the energy content of a volume of stored water changes with changed DH temperature.

The relative variation of the two technologies is presented in Fig. 4d, where 100 °C forward design temperature is used as the base. As seen from the figure, the relative differences of stored heat per volume and capacity of DH network are coinciding.

The temperatures of the DH network forward and return streams were defined to be at the location of the utility unit ($T_f$ and $T_r$) in Fig. 2. In the considered network, the heat is supplied from the utility plant to a transmission network, which transfers the heat to smaller distribution grids.

The heat losses for transmission and distribution were determined individually for 2011 as 2 % and 15 % respectively [19, 20]. By assuming that the losses correspond to transmission network operation at 100 °C and 50 °C for forward and return temperatures, the combined heat transfer characteristics of each individual heat network to the ground was found [28, 29]. Using this assumption, it was possible to estimate the heat losses, as well as the consumer temperature $T_C$ for variations in DH temperatures corresponding to Fig. 1.

The temperature of the soil was estimated as the average of yearly temperature variation for the area (8.8 °C).

Table 1: Current and future temperature sets for DH networks

| Network type | Media | DH forward temperature | DH return temperature |
|---|---|---|---|
| Transmission | $H_2O$ | 110°C | 55°C |
| Old distribution | $H_2O$ | 90°C | 45°C |
| New distribution | $H_2O$ | 70°C | 35°C |
| 4GDH (low limit) | $H_2O$ | 40°C | 20°C |

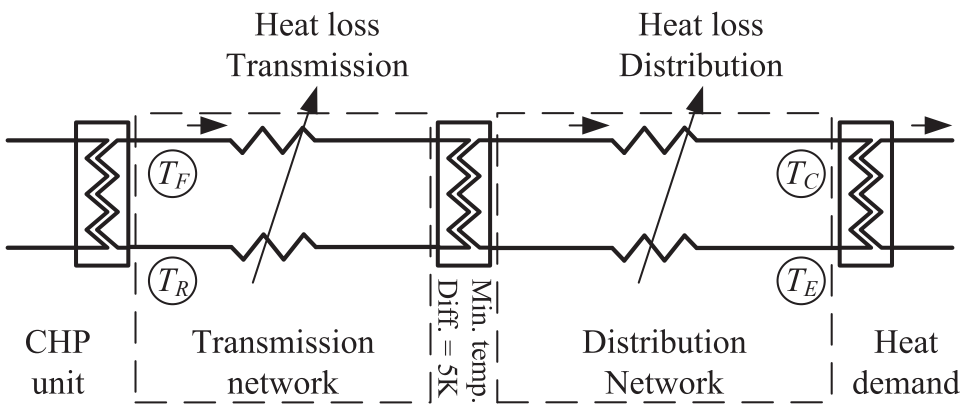


Figure 2: Schematic diagram of DH system with transmission and distribution networks.

### *2.2 Performance of CHP units at changed DH temperatures*

In order to evaluate the effects of changing DH network temperatures, three separate models of CHP plants was programmed in EES. The developed models are:

- Extraction: Extraction type steam turbine (Rankine) cycle.
- Back-pressure: Back-pressure steam turbine (Rankine) cycle.
- Combined cycle: Gas turbine (open Brayton) and steam turbine (Rankine) cycle.

Schematic diagrams of the three considered CHP technologies are presented in Fig. 3. The layout of the three units was modelled to represent specific units in the current utility production.
Besides energy, entropy and mass balances, different, representative expressions were used to establish the impulse balances in different parts of the systems.
For each section of the modelled turbines, a turbine constant accounts for the swallowing capacity of a specific unit:

$$C_T = \frac{\dot{m} \cdot \sqrt{T_{\text{in}}}}{\sqrt{p_{\text{in}}^2 - p_{\text{out}}^2}} \tag{1}$$

where the massflow of working fluid $\dot{m}$, the temperature of entering fluid $T_{\text{in}}$ and pressures at inlet $p_{\text{in}}$ and outlet $p_{\text{out}}$ are used. Once installed, the swallowing capacity should be considered constant throughout the lifetime of the unit. The constant is required to calculate the off-design operation of such units.

#### *2.2.1 Extraction CHP*

In the current energy scenario based on todays Eastern Danish energy system, the Nordpool DK2 area [30], four central extraction CHP units are operated (five in case the reserve unit at Asnæsværket (ASV5) is included), of which three are located within the DH network. The same units are expected to be operating in 2025, although two of the units (which are identical) require overhaul and conversion to biomass fuel.
The model for extraction type steam turbine (Rankine) cycles represent one of these units (AVV1 or AMV3). The model follows the instructions of the proposal for simulator contest of ECOS 2003 [31, 6], where specific information about the temperatures, isentropic efficiencies, temperature differences, auxiliary power consumption and pressure losses are defined. The model used for this analysis corresponded closely to the

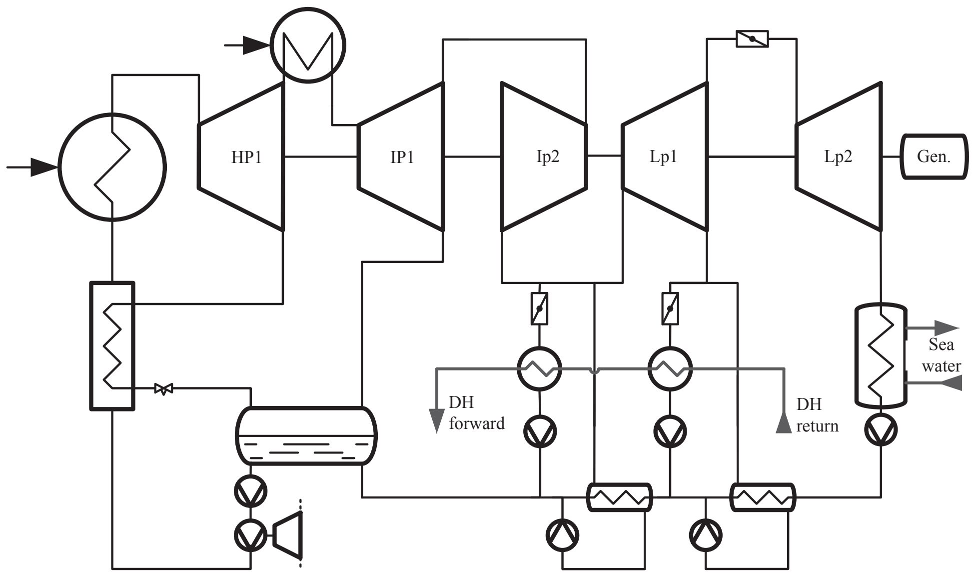


(a) Extraction CHP plant

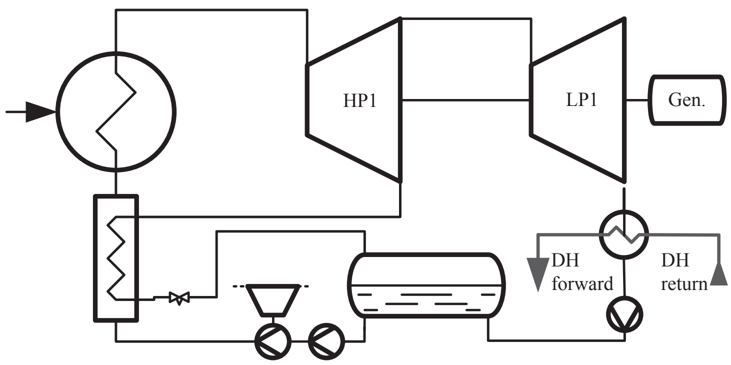


(b) Back-pressure CHP plant

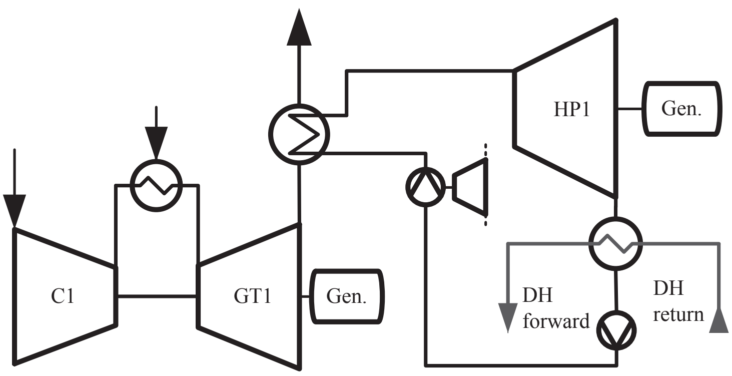


(c) Combined cycle CHP plant

Figure 3: Schematic diagram of the three considered combined heat and power plants.

one used in Ommen et al. [9]. The steam enters the intermediate and low pressure part of the turbine train after expansion in the preceding turbine, IP1, and may be used for power generation or to supply district heating. The output of each product is controlled by adjusting the valves before the low pressure turbines and the district heating heat exchangers.

For each of the valves, a flow characteristic was fixed, in order to account for the pressure losses when the valve is operated between fully open and fully closed. The constant is required to calculate the off-design operation of such units.

$$\dot{V} = \alpha_{\text{valve}} \cdot k \cdot \sqrt{\frac{\Delta p_{\text{valve}}}{\rho_{\text{in}}}}, \tag{2}$$

where $\alpha$ is the flow characteristic, $k$ is the opening degree of the valve and $\Delta p_{\text{valve}}$ is the pressure loss over the valve.

Considering DH temperatures of 100 °C and 50 °C for forward and return temperatures, the model represents a plant with an electric efficiency of 42.0 % at full boiler load and in condensing mode and 34.9 % at full back-pressure mode, respectively. In full back-pressure mode the total energy utilization is 91.5 %.

#### *2.2.2 Back-pressure CHP*

Back-Pressure CHP units are extensively used in Copenhagen today and in future scenarios (see section 2.6). The units are typically fuelled by biomass, or used for waste incineration. A few of the units allow the steam to bypass the turbine, in order to be utilised directly for heat production.

The back-pressure CHP unit was modelled to represent the Amagerværket unit 1 (AMV1), which is a biomass-fuelled unit located centrally in Copenhagen. The component details corresponded to those used for the extraction plant. In the current energy scenario, only a high pressure turbine is installed, as the unit supplies steam to a central network. When the steam network has been phased out (expected before 2025) a low-pressure turbine will be added to the unit.

Considering DH temperatures of 100 °C and 50 °C for forward and return temperatures, the model represents a plant with an electric efficiency of 29.5 % and total energy utilization of 92 %.

#### *2.2.3 Combined cycle CHP*

The combined cycle CHP plant corresponds to the two combined cycle units at Avedøreværket unit 2. For the Rankine cycle, the component details correspond to those used for the extraction plant. Combined cycle units represent a small fraction of the current electricity and heat production, and are expected to play an even smaller role in the system of 2025. Out of the four current units, two will be retired as they are used for the steam network, and the two at AVV2 will be utilised exclusively as electricity reserve measures.

For DH forward and return temperatures of 100 °C and 50 °C respectively, the model represents a plant with an electric efficiency of 51 % and total energy utilization of 85 %.

#### *2.2.4 Performance improvement of CHP technologies from reduction in temperatures of DH network*

The individual models of CHP units were varied according to the district heating temperature levels presented in Fig. 1. In this way, the potential improvements for the individual plants were determined. By assuming, that the models are representative for the individual CHP-plant types, the influence from DH temperatures are found for all considered units in the current and future energy scenarios. The changed performance parameters are presented in Fig. 4a, 4b and 4c for extraction, back-pressure and combined cycle CHP, respectively.

For extraction CHP units, the temperature variations contributed to significant modifications to the electricity efficiency and to the power loss factor by heat extraction $\beta$. For back-pressure units the electricity efficiency was significantly changed. For both extraction and back-pressure CHP units, minor impact was experienced for the total energy utilization of the unit.

For the combined cycle technology, the electric efficiency has changed with variation of DH temperature. Opposed to the above-mentioned technologies, the alteration of DH temperature affects the total efficiency significantly, although less than the corresponding change in electrical efficiency.

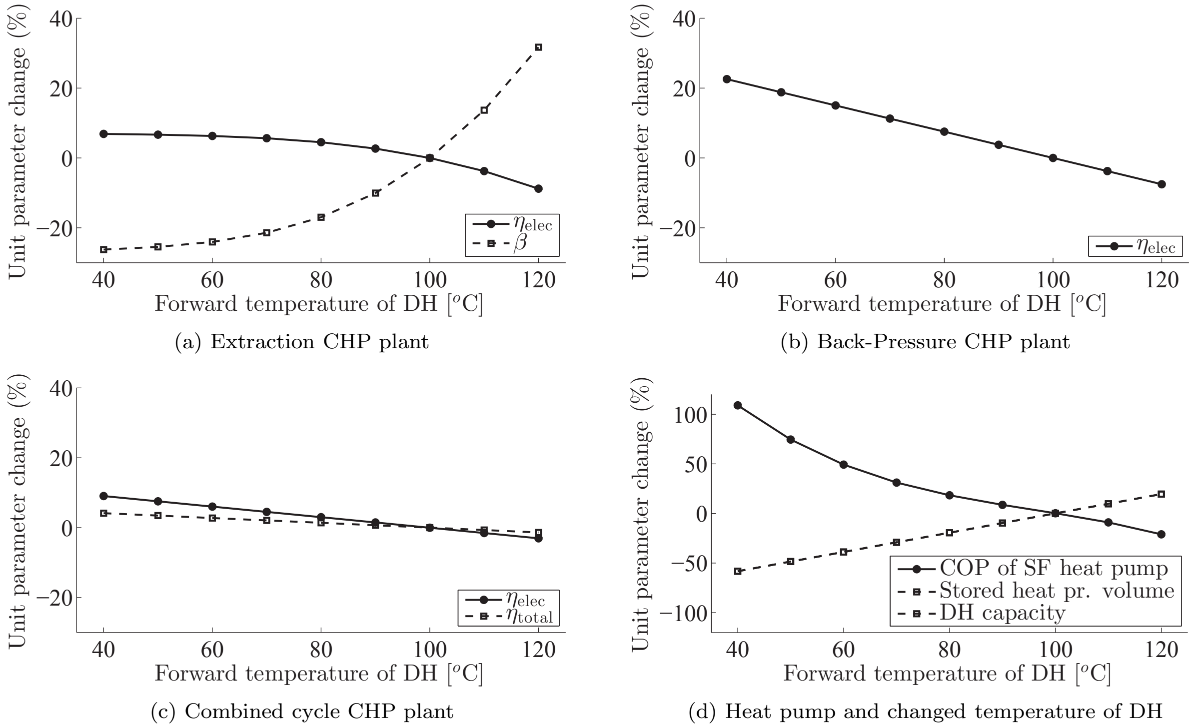


(a) Extraction CHP plant
(b) Back-Pressure CHP plant
(c) Combined cycle CHP plant
(d) Heat pump and changed temperature of DH

Figure 4: Changed performance parameters of three CHP types, HP and changed temperatures in DH network when design conditions (100 °C forward temperature) are altered to off-design operation.

### *2.3 Heat pumps in DH*

In Ommen et al. [9] five possible heat pump configurations in DH networks are analysed. The operational performance of the configurations are investigated based on four key performance factors, which are the coefficient of performance, the coefficient of system performance, the volumetric heating capacity and the cost of fuel.

The SF configuration was utilised for the present analysis. In this configuration the sink DH stream is heated from the temperature of the return line to that of the forward stream. The main advantage of the SF configuration is that this configuration allows operation independently of other technologies. A schematic diagram of a single stage vapour compression heat pump is presented in Fig. 5.

The performance of the HP was evaluated based on four variables and fixed temperature differences for both evaporator and condenser. The utilised variables were: the temperature of the sink process stream leaving the condenser $T_{\text{sink}}$, the temperature of the source $T_{\text{source}}$ and the process stream temperature variation from inlet to outlet in both heat exchangers ($\Delta T_{\text{sink}}$ and $\Delta T_{\text{source}}$). Both the sink temperature, and the variation of the sink was determined for a SF configuration HP as the forward temperature of DH, or the difference between DH forward and return in Fig. 1, respectively.

The temperature of the source is dictated by the type and location of the installation [32]. By using a DH network, large installations can be located near heat sources of elevated temperatures (compared to ambient conditions), such as sewage water, industrial waste heat, power plant stack gasses etc. Most of these heat sources tend to have a low yearly temperature variation and a finite heat capacity rate of the stream. In some cases the heat source can also be ocean or lakes where yearly variation in temperature would be expected.

The performance of the considered heat pump was calculated using constant efficiencies for compressor and electrical motor, as well as fixed temperature differences in the heat exchangers. The used values for heat source and performance of equipment are presented in Table 2.

For DH forward and return temperatures of 100 °C and 50 °C respectively, the HP model represents a

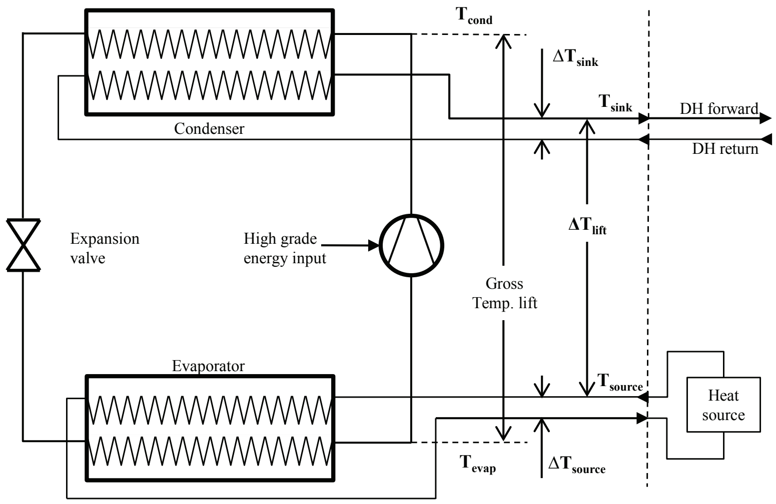


Figure 5: Schematic diagram of a single stage heat pump system for DH (configuration SF)

Table 2: Operational parameters for SF configuration HP

| | Value | Unit | Designation |
|---|---|---|---|
| Type | R134a | - | Working fluid |
| Efficiency | 0.8 | - | Compressor isentropic efficiency |
| | 0.95 | - | Electric motor efficiency |
| Temperature | 20 | °C | Temperature of heat source |
| | 10 | K | Temperature variation of heat source |
| | 5 | K | Evaporator superheat |
| | 5 | K | Minimum pinch point in heat exchangers |

unit with a COP of 2.97 (-) including electric motor efficiency (3.12 (-), if only the thermodynamic cycle is considered).

### *2.4 DH booster heat pump*

For supply of hot tap water, two constraints are to be respected, considering the Danish DH case. The requirements of the Danish building standard must be met [33], where hot tap water is utilised at two temperature levels 45 °C and 40 °C, respectively. Additionally, a main concern is the issues related to the Legionella bacterium. To avoid bacteria growth, the hot tap water must either exceed a predefined temperature limit, where the bacteria can no longer exist when stored, or the tap water is not to be stored after being heated.

Two HP booster integration schemes were identified, corresponding to the schemes presented in Fig. 6a and 6b. In Ommen and Elmegaard [23] various specific configurations are investigated and compared based on their exergy efficiency. It is found that a heat pump on the primary side of the hot tap water heat exchanger, is superior in terms of COP and exergy efficency at almost all temperature configurations of low temperature DH. The considered configuration is presented in Fig. 6c.

In case the temperature of the DH network at the location of the consumer (in Fig. 2) is lower than 55 °C, it is assumed that the hot tap water constitutes a fixed share of DH heat demand. The share was determined

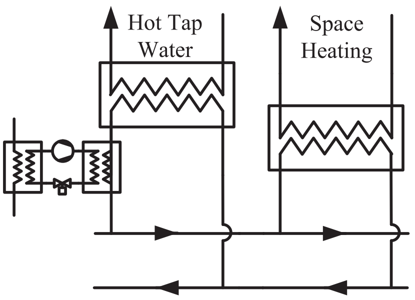


(a) Heat pump on primary side of the tap water heat exchanger

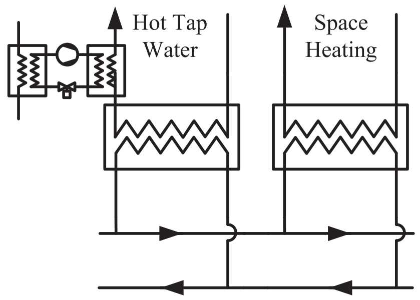


(b) Heat pump on secondary side of the tap water heat exchanger

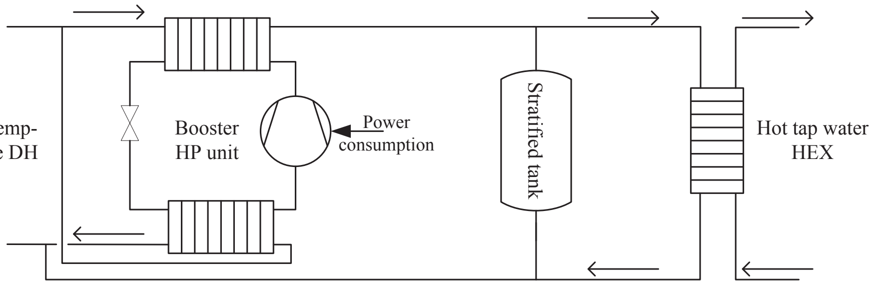


(c) Specific layout of DH booster HP unit

Figure 6: Two DH booster HP integration schemes.

by assessing the heat demand of the individual area (without heat losses) during the periods of the year where space heating is not needed. The remaining part of the supplied heat is utilised for space heating, and it was assumed that this fraction did not require boosting of the temperature.
For district heating consumer forward temperature of 40 °C and return temperature of 22 °C, the model represents a unit with a COP of 5.6 (-) and a power consumption of 0.066 kWh per kWh of hot tap water. For a forward temperature approaching 55 °C, the heat load is reduced and the COP of the unit increases. Thus at 55 °C the electricity consumption for boosting tap water temperatures becomes zero.

### *2.5 Heat and power system model*

A detailed system model was developed for calculation of the economic and environmental impact of integrating heat pumps in an energy system with a high share of CHP-plants and intermittent electricity production from renewable technologies, e.g. wind turbines. The result was a validated heat and power system model, which features detailed representation of CHP technology as well as detailed representation of different heat pump technologies and integration possibilities [13].
The optimal production cost for the combined system can be achieved by minimisation of consumer cost for electricity and heat in daily auctions on hourly basis [34]. The optimal daily market clearances are then added for the duration of the year. When considering a system where capital cost can be considered as sunk cost, the objective function can be written as 3.

$$\min \left[ \sum_{t \in \mathcal{T}} \left( \sum_{i \in \mathcal{I}} (\dot{C}^{\mathrm{CHP}}_{i,t}) + \sum_{h \in \mathcal{H}} (\dot{C}^{\mathrm{boiler}}_{h,t}) + \sum_{g \in \mathcal{G}} (\dot{C}^{\mathrm{HP}}_{g,t}) + \sum_{f \in \mathcal{F}} (\dot{C}^{\mathrm{Other}}_{f,t}) + \sum_{j \in \mathcal{J}} (\dot{C}^{\mathrm{import}}_{j,t} - \dot{C}^{\mathrm{export}}_{j,t}) \right) \right] \tag{3}$$

Where $\dot{C}$ is the total cost rate of production at the individual plant. The CHP units in the system are indexed by $\mathcal{I}$, boilers by $\mathcal{H}$, heat pumps by $\mathcal{G}$ and other heat and/or electricity production by $\mathcal{F}$. The neighbouring energy markets are indexed by $\mathcal{J}$.

It was assumed, that electricity and heat production of small-scale decentralized CHP-plants and intermittent electricity production from wind turbines are independent of the electricity cost in the individual hour. Using this assumption, the production profile of such units can be obtained from historical data.
The objective function shown in Eq. 3 was subject to a number of economic and technical constraints, of which the most important ones are presented and explained in appendix A. The economic constraints related to taxation are autonomous for each country, and are thus not presented in detail here. We refer to [13] for further information. The cost rates include all costs associated with utility production (e.g. fuel, taxes and subsidies) at the specific plant. In order to ensure the competitive conditions for import and export of electricity across taxation borders, the taxes for electricity are placed on the consumption. This is opposite to taxation for fuel, which is closely linked to the production.
The detailed representation of the CHP units includes various features which are briefly mentioned below:

- Four types of power plant units possible: Back-pressure, extraction, gas turbines/combined cycle or condensation.
- Limitation for hourly ramp rates and minimum technical production limits.
- Reduction in electricity production efficiency at part-load operation, which is specified individually for each unit.
- Startup and shutdown costs corresponding to size and type of unit
- Extraction technology represented by two power loss factors by heat extraction ($\beta^1, \beta^2$) depending on production above or below the "no-loss" point [7].
- Production at specific units can be prioritised, e.g. waste incineration.
- Availability (to market) is set individually for all units. For validation these data were obtained from urgent market messages from Nord Pool Spot [35].
- Different Danish taxation schemes for heat production are preprogrammed for each unit.
- Steam bypass of turbine possible for back-pressure CHP-units.
- Minimum available manual and frequency reserves are included for the total system, and technical limitations of reserves may be specified individually for each unit.
- Specific units may produce at higher capacity than their rating (overload) at reduced efficiency.

### *2.6 Current and future energy scenarios for Copenhagen*

For each of the thermal CHP units in the current and planned utility system, specific information regarding capacity and efficiency, cost of fuels and maintenance, as well as capacities and consumption of the network were available online from various sources [36, 37, 38, 39, 40, 14].
In this way it was possible to derive the plant characteristics for current (Table 3a) and future (2025) energy scenario (Table 3b). Most of the data in the table is referring directly to the operational parameters of the individual units, but the table also includes fuel cost for 2011 and 2025 using historical prices or prognoses [38]. It should be noted that both electric efficiency and energy utilization were calculated for the plant in back-pressure operation mode.
The capacity and demand profiles, as well as planned changes, of DH networks in 2012 and 2025 were based on information from CTR, HOFOR and VEKS [14]. Changes to the demand, capacity of decentral CHP, on- and offshore wind turbines, photovoltaics and spot-prices for electricity in 2025 were available from Energinet.dk [38].
As the process of converting old steam networks to water-based networks is ongoing, the heat demand for water-based networks increases its demand faster than that which can be related to the heat demand from new areas. In the current scenario a number of units produces heat for the steam network, and is thus not

Table 3: Thermal power plant unit characteristics for central power plants and waste inceneration plants in DK2 bidding area.

(a) Current (2011) energy scenario

| | Fuel type | Cost fuel (€/GJ) | Type | Priority | Turb. byp. | $\eta_{\text{elec}}$ (-) | $\eta_{\text{total}}$ (-) | $\beta^1$ (-) | $\beta^2$ (-) | Ramp rate (-) | Min. load (-) | Man. reserve (-) | Freq. reserve (-) | $\eta_{\text{elec}}$ reduction (%) | Boiler capacity (MW) |
|---|---|---|---|---|---|---|---|---|---|---|---|---|---|---|---|
| AMV1 | bio/straw | 9.4 | Backp. | | X | 0.20 | 0.92 | | | 0.25 | 0.50 | | 0.05 | 0.08 | 350 |
| AMV3 | coal | 3.3 | Extr. | | | 0.35 | 0.89 | 0.14 | 0.10 | 0.25 | 0.50 | | 0.05 | 0.08 | 595 (+75) |
| HCV4 | nat. gas | 5.9 | Backp. | | X | 0.11 | 0.82 | | | 0.25 | 0.45 | 0.03 | 0.05 | 0.08 | 157 |
| HCV7 | nat. gas | 5.9 | Backp. | | X | 0.26 | 0.89 | | | 0.25 | 0.45 | 0.03 | 0.05 | 0.08 | 285 |
| HCV8 | nat. gas | 5.9 | CC | | | 0.20 | 0.89 | | | 1.00 | 0.55 | 0.05 | 0.10 | 0.16 | 127 |
| SVM7 | nat. gas | 5.9 | CC | | | 0.23 | 0.92 | | | 1.00 | 0.50 | 0.05 | 0.10 | 0.16 | 275 |
| AMF1 | waste | 4.0 | Backp. | X | X | 0.21 | 0.83 | | | 0.25 | 0.70 | | | 0.08 | 132 |
| AVV1 | coal | 3.3 | Extr. | | | 0.35 | 0.89 | 0.14 | 0.10 | 0.25 | 0.50 | 0.03 | 0.05 | 0.08 | 595 (+75) |
| $\text{AVV2}_{\text{B1}}$ | bio | 9.9 | Extr. | | | 0.36 | 0.92 | 0.18 | 0.12 | 0.25 | 0.45 | 0.03 | 0.05 | 0.08 | 805 |
| $\text{AVV2}_{\text{B2}}$ | straw | 8.0 | Extr. | | | 0.34 | 0.91 | 0.16 | 0.12 | 0.25 | 0.45 | | | 0.08 | 100 |
| $\text{AVV2}_{\text{cc1}}$ | nat. gas | 5.9 | CC | | | 0.51 | 0.85 | 0.11 | 0.11 | 1.00 | 0.55 | 0.05 | 0.10 | 0.16 | 135 |
| $\text{AVV2}_{\text{cc2}}$ | nat. gas | 5.9 | CC | | | 0.51 | 0.85 | 0.11 | 0.11 | 1.00 | 0.55 | 0.05 | 0.10 | 0.16 | 135 |
| KARA5 | waste | 4.0 | Backp. | X | X | 0.17 | 0.80 | | | 0.25 | 0.70 | | | 0.08 | 65 |
| VF5 | waste | 4.0 | Backp. | X | | 0.13 | 0.82 | | | 0.25 | 0.70 | | | 0.08 | 90 |
| VF6 | waste | 4.0 | Backp. | X | | 0.19 | 0.82 | | | 0.25 | 0.70 | | | 0.08 | 105 |
| ASV2 | coal | 3.3 | Extr. | | | 0.31 | 0.88 | 0.18 | 0.15 | 0.25 | 0.20 | 0.03 | 0.05 | 0.08 | 368 |
| ASV5 | coal | 3.3 | Extr. | | | 0.26 | 0.88 | 0.18 | 0.15 | 0.25 | 0.40 | 0.03 | 0.05 | 0.08 | 1750 |
| KYB1 | oil | 11.9 | Elec. only | | | 0.33 | 0.33 | | | 0.60 | 0.48 | 0.03 | 0.05 | 0.08 | 790 |
| KYB2 | oil | 11.9 | Elec. only | | | 0.33 | 0.33 | | | 0.60 | 0.48 | 0.03 | 0.05 | 0.08 | 790 |

(b) Future (2025) energy scenario

| | Fuel type | Cost fuel (€/GJ) | Type | Priority | Turb. byp. | $\eta_{\text{elec}}$ (-) | $\eta_{\text{total}}$ (-) | $\beta^1$ (-) | $\beta^2$ (-) | Ramp rate (-) | Min. load (-) | Man. reserve (-) | Freq. reserve (-) | $\eta_{\text{elec}}$ reduction (%) | Boiler capacity (MW) |
|---|---|---|---|---|---|---|---|---|---|---|---|---|---|---|---|
| AMV1 | bio/straw | 8.9 | Backp. | | X | 0.30 | 0.92 | | | 0.25 | 0.50 | | 0.05 | 0.08 | 350 |
| AMV3 | bio | 9.9 | Extr. | | | 0.34 | 0.89 | 0.14 | 0.10 | 0.25 | 0.50 | | 0.05 | 0.08 | 640 |
| AMF1 | waste | 4.0 | Backp. | X | X | 0.21 | 0.99 | | | 0.25 | 0.70 | | | 0.08 | 203 |
| FLIS1 | bio | 9.9 | Backp. | | X | 0.20 | 0.99 | | | 0.25 | 0.45 | | | 0.08 | 150 |
| AVV1 | bio | 9.9 | Extr. | | | 0.34 | 0.89 | 0.14 | 0.10 | 0.25 | 0.50 | 0.03 | 0.05 | 0.08 | 640 |
| AVV2 | bio | 9.9 | Extr. | | | 0.36 | 0.92 | 0.18 | 0.12 | 0.25 | 0.45 | 0.03 | 0.05 | 0.08 | 960 |
| AVV3 | straw | 5.7 | Extr. | | | 0.34 | 0.91 | 0.16 | 0.12 | 0.25 | 0.45 | | | 0.08 | 125 |
| KARA5 | waste | 4.0 | Backp. | X | X | 0.17 | 0.80 | | | 0.25 | 0.70 | | | 0.08 | 65 |
| KARA6 | waste | 4.0 | Backp. | X | X | 0.22 | 0.99 | | | 0.25 | 0.70 | | | 0.08 | 82 |
| VF5 | waste | 4.0 | Backp. | X | | 0.12 | 0.99 | | | 0.25 | 0.70 | | | 0.08 | 90 |
| VF6 | waste | 4.0 | Backp. | X | | 0.18 | 0.99 | | | 0.25 | 0.70 | | | 0.08 | 105 |
| VF7 | waste | 4.0 | Backp. | X | | 0.27 | 0.99 | | | 0.25 | 0.70 | | | 0.08 | 102 |
| KKV7 | bio | 9.9 | Backp. | | X | 0.18 | 0.90 | | | 0.25 | 0.45 | | | 0.08 | 45 |
| KKV8 | bio | 9.9 | Backp. | | X | 0.25 | 0.90 | | | 0.25 | 0.45 | | | 0.08 | 55 |
| ASV2 | coal | 3.2 | Extr. | X | | 0.31 | 0.88 | 0.18 | 0.15 | 0.25 | 0.20 | 0.03 | 0.05 | 0.08 | 368 |
| KYB1 | oil | 16.0 | Elec. only | | | 0.33 | 0.33 | | | 0.60 | 0.48 | 0.03 | 0.05 | 0.08 | 790 |
| KYB2 | oil | 16.0 | Elec. only | | | 0.33 | 0.33 | | | 0.60 | 0.48 | 0.03 | 0.05 | 0.08 | 790 |

Table 4: Four different cases for analysis of impact to system performance from lowering DH temperatures

| | Energy scenario | Capacity dependent on temperature of DH |
|---|---|---|
| Case #1 | 2011 | no |
| Case #2 | 2011 | yes |
| Case #3 | 2025 | no |
| Case #4 | 2025 | yes |

effected by changes to the network temperature for water based DH systems. The units are AMV1, HCV4-8 and SMV7.
The scenarios were named as four different cases, Case #1-4. The details of the cases are presented in table 4. The difference between case #1 and #2 as well as case #3 and #4 is the use of temperature dependency for capacity constraints in the DH network, as well as temperature dependency for storage systems. The objective of including case #2 and #4 was to show the effects of the temperature dependency in the specific case that no further investments were made to the transmission network or to the storage facilities. This can be seen as a conservative estimate.
The objective of case #1 and #3 was to analyse the effects of lowering temperature, with similar capacity constraints as proposed for the traditional temperature levels. This assumption reflects that some critical network and storage capacity constraints in the transmission network can be low cost changes, compared to the magnitude of investments for the remaining system. Such investments would further imply additional work to DH pumps, due to increased volume flow, which is not included for the analysis. This may thus be seen as a high estimate.
The four energy system cases were further expanded by introduction of a significant capacity of central SF configuration heat pumps (as presented in section 2.3). For each of the four cases the system was analysed without introduction of HP capacity, as well as a case with 200 MW capacity installed in the transmission network of the DH system (denoted "W/HP" for cases with HP installed). The installed capacity was divided equally at two locations, namely the location of Amagerværket (AMV) and Avedøreværket (AVV).
Carbon emissions for heat and electricity production in CHP plants were calculated based on the 125 % method for heat, assuming that heat is produced at 125 % efficiency, whereas the remaining part correspond to electricity production [41]. Other methods are also utilised for splitting contributions, such as 200 %, energy basis or quality (exergy) of content. Carbon emissions from combustion of fuel correspond to the Danish Energy Agency [40]

## 3 Results

The various energy system scenarios were compared based on six different parameters. The parameters were: Combined system cost, $CO_2$-emissions from heat and electricity individually, primary energy consumption, net imported electricity and the production ratio between electricity and heat in the extraction CHP units. The calculated results represent the entire bidding area, except for carbon emissions of heat, where the results represent the emissions in the Greater Copenhagen DH area.
The results of the analysis were calculated as relative differences, compared to the energy scenario base case - either state of the art (2011) or compared to the future scenario (2025) as presented in [14]. This implies, that the results of a specific calculation (e.g. Case #1 at 60 °C) correspond to the relevant scenario (2011) at DH network design temperature of 100 °C. Each of the six calculated system parameters are presented in table 5 for both current and future energy scenario.
Although only separated by 14 years, the two energy system scenarios are quite different in terms of cost and carbon emissions. The main reason for the reductions in primary energy use and net import of electricity in 2025 was the significant increase in intermittent electricity production.
The reason for the discrepancy between the calculated emissions and the previously mentioned zero carbon emission goal, was the difference in imposition for carbon expenditure for waste as a fuel. In *Heat plan*

Table 5: Results of energy scenarios base case (100 °C) for six system parameters

| Parameter | Unit | 2011 scenario | 2025 scenario |
|---|---|---|---|
| Total system cost | $10^8$ € | 5.16 | 5.95 |
| Heat $CO_2$-emission | kg/MWh | 0.13 | 0.05 |
| Electricity $CO_2$-emission | kg/MWh | 0.36 | 0.15 |
| Primary energy use | $10^7$ GJ | 8.42 | 7.38 |
| Net. Imported Electricity | $10^6$ MWh | 2.09 | 1.10 |
| Extr. CHP prod. ratio | % | 0.00 | -2.20 |

*Greater Copenhagen* a significant effort is placed for recycling the carbon constituents from waste [14], whereas the performed calculations in this paper assume similar carbon composition as that of today. The influence to $CO_2$-emission for exported electricity corresponds to the overall emissions from electricity, which thus influences not only the specific bidding area, but also to a limited extent the emissions of neighbouring transmission networks.

### *3.1 Current energy scenario*

The results for case #1 and #2 are presented in Fig. 7 relative to the 2011 scenario. For case #1, system cost and $CO_2$-emissions are presented in Fig. 7a, whereas primary energy use, net imported electricity and extraction CHP production ratio are presented in Fig. 7b. For case #2, similar parameters are presented in Fig. 7c and 7d respectively. The results of DH temperature variations for the base case (without HPs) is presented in black color, whereas results representing configurations with the additional installed heat pump capacity, are presented in gray.

By reducing DH temperatures for Case #1 (Fig. 7a), the consumer cost were reduced up to approximately 2.8 %, and emissions by approximately 1 % and 6.4 % for electricity and heat respectively. The performance improvements were consequences of the increased electricity production efficiency at CHP plants, as well as reduction in heat losses from the network.

Both system cost and carbon emissions from electricity reached a minimum at 60 °C, whereas the minimum emissions for heat were found for forward temperatures of 50 °C. The minimum can be explained by the utilisation of additional electricity to increase the temperature of the hot tap water, when the consumer temperature decreases below the set value of 55 °C.

The electricity and heat demands are similar for all results corresponding to a specific energy scenario, and thus also the interdependency for the specific CO2 emissions for the overall emissions.

By integration of the considered central HP capacity the cost was further reduced. For the reference temperature level (100 °C) a reduction in system cost of 1.2 % was possible, with a corresponding reduction in emissions for heat of 3.6 %. $CO_2$ emissions for electricity was reduced slightly. The trend for system cost for a system with HPs resembles that of the base case, but with an offset in favour of the HP case of approximately 2 percentage-points. The combination of reduction in DH temperatures and integration of central HP capacity in the network resulted in large reductions of $CO_2$ emissions for heat. The maximal reduction was 19 %, which was found for DH forward temperature of 40 °C. For forward temperatures below 80 °C the $CO_2$ emissions for electricity was increased compared to the system without HP capacity (up to 2 % increase).

It was found that both primary fuel usage and import of electricity decreased when decreasing DH temperatures for case #1 (Fig. 7b). For the case with HP integration, the primary energy usage decreased further, whereas the net import of electricity increased significantly. Such results suggest that the constrained production of CHP units was reduced by integrating HPs. This presumption was further supported by increased electricity production ratio of extraction CHP plants in the case with HPs compared to case #1, and correspond to the increased $CO_2$ emissions for electricity, as less heat was produced from thermal units, which shifts carbon emissions from the consumed fuel towards electricity. The increased production

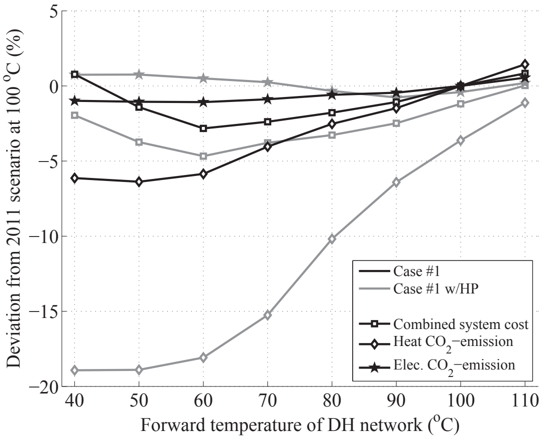


(a) Case #1: System cost and $CO_2$ emissions

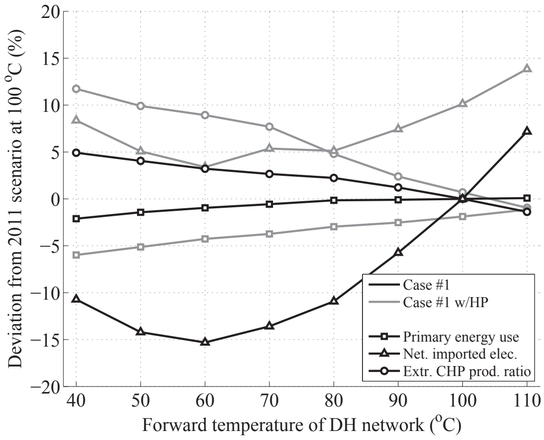


(b) Case #1: Primary energy use, net import of electricity and extraction CHP prod. ratio

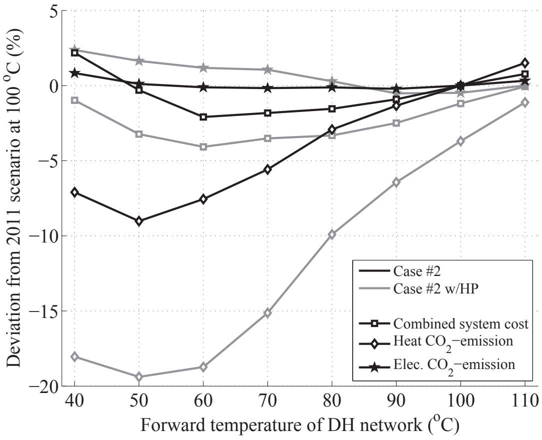


(c) Case #2: System cost and $CO_2$ emissions

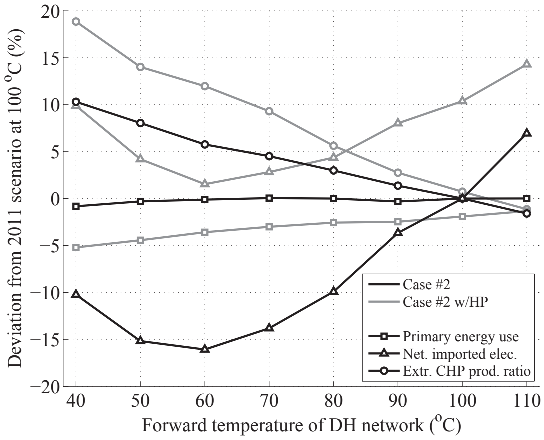


(d) Case #2: Primary energy use, net import of electricity and extraction CHP prod. ratio

Figure 7: Impact to key parameters for lowering DH network temperature for Case #1 and #2 and with integration of 200 MW central HP capacity

ratio of extraction CHP plants in case #1 (without HP) may be explained by the increase in back-pressure efficiency from reduction in DH temperatures.

For case #2 (capacity and storage constraints according to change in DH temperature levels) the obtained results resemble those presented above. Comparing Fig. 7a and 7b with 7c and 7d respectively, it was found that trends are similar at high DH temperatures, whereas the performance improvements at low DH forward temperatures were reduced. The impact was increasingly significant at forward temperatures below 60 °C. The potential benefits at the temperature levels of maximal reductions from case #1 were reduced, but even with capacity constraints in place, the benefit was significant. As an example, the combined system cost reduction was changed from 2.8 % to 2.1 % for the system without HP integration, and reductions in carbon emissions for the system with HPs integrated are even slightly increased. A significant difference was found for the production ratio of extraction CHP plants, which at low forward temperatures increased approximately 5 % for the system without HP, and 6 % for the system with integration of HPs. The difference was particularly large for DH temperatures of 40-60 °C. This could suggest that the production ratio was changed due to limited network capacity at periods with high heat consumption.

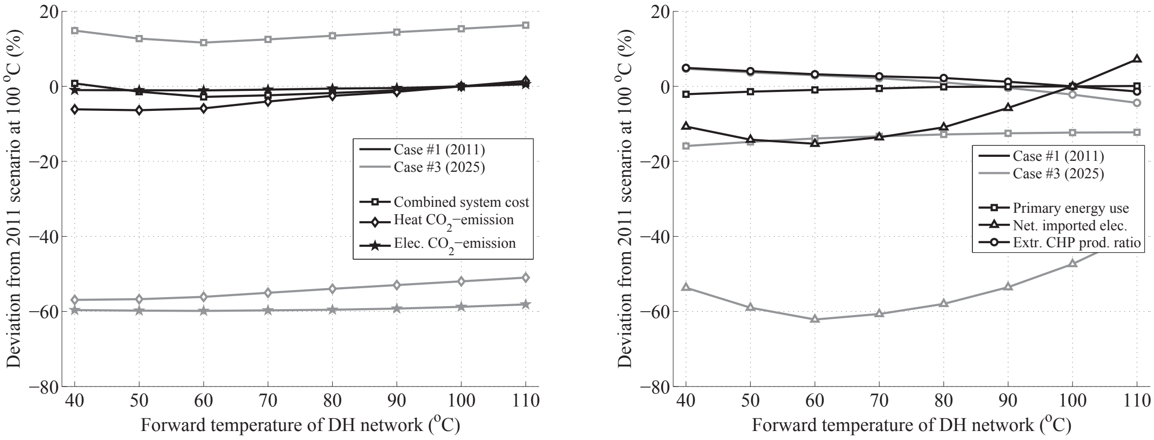


(a) Case #1 and #3: System cost and $CO_2$ emissions

(b) Case #1 and #3: Primary energy use, net import of electricity and extraction CHP prod. ratio

Figure 8: Comparison of key parameters for current and future energy system scenarios

### *3.2 Comparison of the two energy scenarios*

The two reference scenarios (2011 and 2025) are compared in Fig. 8. The results of both scenarios were calculated on the basis of the 2011 scenario (in table 5). Variations from the investigated parameters are presented in black colour for case #1, and by gray curves for case #3.

The case #1 data for cost and $CO_2$-emissions in Fig. 8a, as well as primary fuel usage and import in Fig. 8b, are similar data as those presented in Fig. 7a and 7b, respectively. Compared to case #1, case #3 presented significantly increased system cost (typically around 14-15 % increase) but at the same time significantly reduced heat and electricity $CO_2$ emissions. The reductions in emissions were minimum 52 % for heat and 58 % for electricity.

From Fig. 8b it is found, that case #3 implied a significantly lower net import of electricity (between 40 and 50 %), and lower consumption of primary energy (approximately a reduction of 14 %). The reduction was due to a large increases of intermittent electricity in the future scenario. This was obtained without significantly affecting the production ratio of the extraction plants compared to todays operation.

The impact of changing DH temperatures on the performance of the two cases was shown to be equal in magnitude and experience similar trends at various temperature levels.

### *3.3 2025 energy scenario*

Results for future scenario cases #3 and #4 are presented in Fig. 9. The reference data (black) of Fig. 9a and 9b, corresponds to the gray curves presented in Fig. 8a and 8b, respectively.

The maximal reduction in system cost, by decreasing the DH temperatures, was 3.2 % for case #3, and a reduction of 6 % when the considered additional HP capacity was integrated. For both cases this was marginally higher savings, than those presented for case #1. For case #3 with HP, the savings at forward temperatures of 50 °C was similar to that of 60 °C. The gain from integrating HP technology in low temperature DH in terms of cost was larger in 2025 low temperature scenarios, compared to 2011. For the case of 50 °C, the gain of central HP units were at a magnitude, where the technology compensates for the additional electricity consumption at the consumer booster HP.

The gain in terms of $CO_2$ emissions of lowering DH temperatures for case #3 were small, considering systems with or without central HP integration. The maximal reduction was for heat, which was 5.8 and 7.2 % respectively, but as the base scenario was already significantly reduced, the actual reductions were low. From Fig. 9b it was found that net imported electricity was significantly reduced, with a minimum at -24 to -28 % for 60 - 70 °C depending on whether or not HP capacity was included.

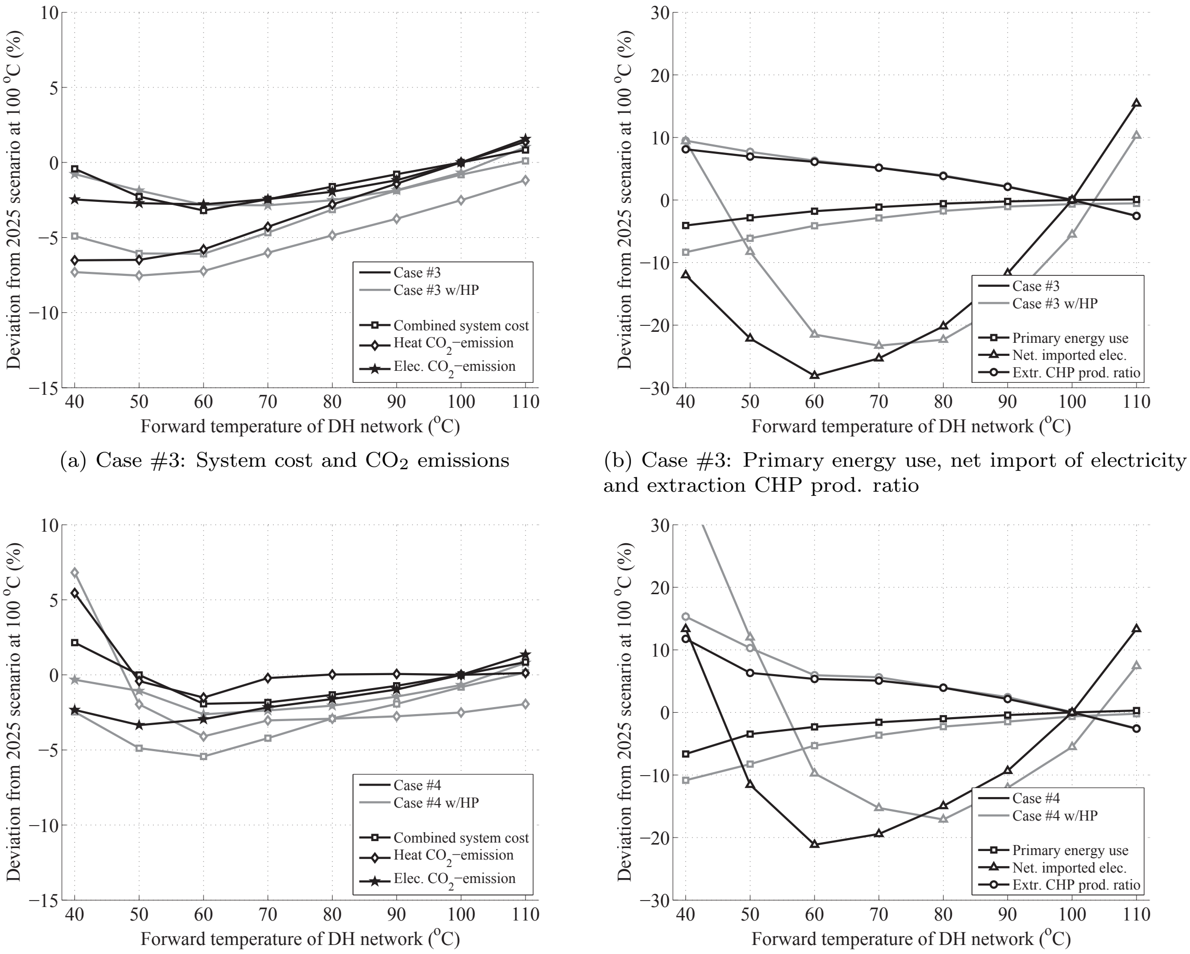


(a) Case #3: System cost and $CO_2$ emissions

(b) Case #3: Primary energy use, net import of electricity and extraction CHP prod. ratio

(c) Case #4: System cost and $CO_2$ emissions

(d) Case #4: Primary energy use, net import of electricity and extraction CHP prod. ratio

Figure 9: Impact to key parameters for lowering DH network temperature for Case #3 and #4 and with integration of 200 MW central HP capacity

As for the similarities between case #1 and #2, corresponding characteristics were found for the differences between case #3 and #4. The effects of DH temperature capacity constraints were large at DH temperature levels below 60 °C. A difference for the future scenario was that a reduction in carbon emissions was not achieved for case #4 at DH temperatures between 70 and 110 °C.

### *3.4 Parametric analysis*

A detailed parametric analysis is presented for four significant input parameters, and analysed for three of the six presented parameters, as well as HP operation hours for the two units. The parametric analysis was performed for the 2025 energy scenario, case #4 w/HP, and is presented in Fig. 10 with variations of ± 20 % of the individual input parameters. The results were calculated as relative to DH network temperatures of 100 °C for 2025 scenario.

The four considered input parameters are presented below:

- Mean spot price for bidding area. Capacity of interconnections remain as specified by Energinet.dk [38].

- Biomass fuel cost.
- Production of electricity from residual technologies. This parameter is for both intermittent sources as well as decentral CHP units.
- The COP of the considered HP.

In Fig. 10a the influence of the four input parameters is presented for the combined system cost. It was found that the spot price, biomass fuel cost and the changes in production of residual electricity technologies affected the results with similar magnitude: approximately 5 to 7 % changed cost for a 20 % change in input parameter. Changes to HP COP influenced the cost of the system to a minor degree.
For carbon emissions from electricity, the chosen input parameter of biomass fuel cost was highly sensitive. A reduction of 14 % on carbon emissions for 20 % reduction in fuel cost was experienced, according to Fig. 10b. The influence was not as significant if the fuel cost was increased. Minimal changes were found for changes to $CO_2$ emissions from heat (Fig. 10c), where the fuel cost of biomass again was the most sensitive. In Fig. 10d heat pump operation hours were presented. It was shown, that one unit (the one located at Avedøreværket) experienced significantly less operation hours than the sibling (located at Amagerværket). This was included to show that for case #4 w/HP, at 70 °C, the DH network capacity constraints were a significant limitation to the considered technologies, especially for the marginal cost unit of the network capacity.

## 4 Discussion

In the analysis, the influence of varying DH temperatures for several different utility technologies was examined. This was done in order to establish the potential for reductions in cost and primary fuel consumption. In such large systems with many cooperating units, minor misrepresentation for individual technologies can have affected the production distribution, but not significantly influenced the total consumer cost, carbon emissions or total primary fuel use. The litterature study revealed no similar studies or analysis, and comparison with relevant literature was thus not possible.
The energy system model which was utilised for the analysis has been validated against historical data of 2011. The scenario of the current energy system was based directly on the validated calculation. The future energy scenario was based on a prognosis of demand and planned energy system changes such as design data for new units [38, 14].
The impact of lowering temperatures for utility technologies in the network were calculated based on a series of thermodynamic models. Due to lack of data, only the model for the extraction CHP plant was validated (against Elmegaard and Houbak [6]), but the remaining models was verified for operation within the considered temperature span for DH. The model for the DH booster HP configuration was previously published and the technology is currently close to commercially available [42].
Several of the findings (e.g. Fig. 7 and 9) suggested choosing temperatures at 60 °C, as this technically is the optimal temperature for achieving low operation cost. In the analysis, the investment cost related to changes in the system were not included, which likely would change recommendation towards higher temperatures. Additionally, at 60 °C forward temperatures, the consumer temperature was below 55 °C, which thus required DH booster HP units in all dwellings. As the reduction in terms of cost and emissions were low from utilising temperatures above this investment limit, forward temperatures of e.g. 70 °C would likely result in increased relevance for the consumer.
The presented results may be seen as case specific, as they represent the specific generation technologies, demand curves and capacity constraints of the Greater Copenhagen network. But, as shown in the analysis, the two energy scenario cases result in quite similar trends for development in terms of cost, carbon emissions and primary fuel consumption. Thus, it is expected that similar trends would be representative for other large networks.
The transmission network was included in the calculation, due to the impact of such constraints to cost reductions or energy efficiency in the current system. By changing the DH network temperatures further capacity constraints may occur, e.g. in the distribution network. Such information was not available, and

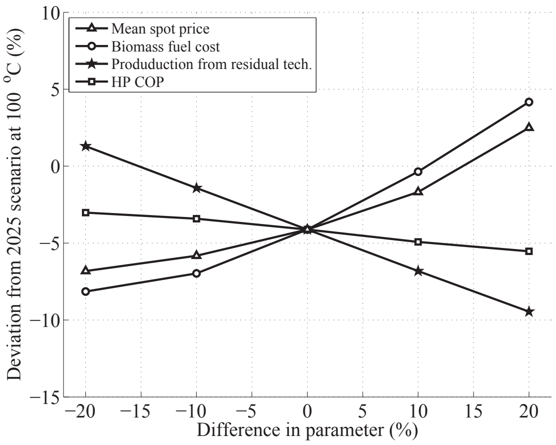


(a) Case #4 w/HP: Combined system cost

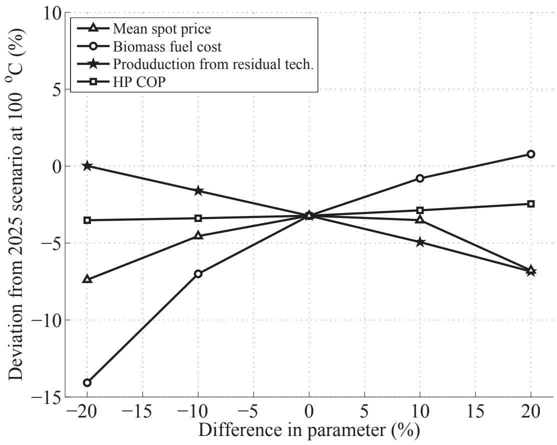


(b) Case #4 w/HP: $CO_2$-emissions of electricty

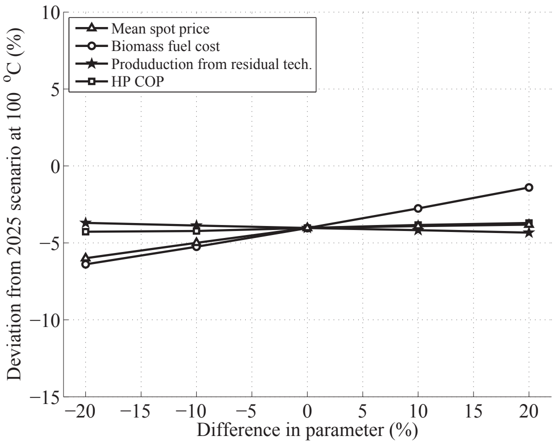


(c) Case #4 w/HP: $CO_2$-emissions of heat

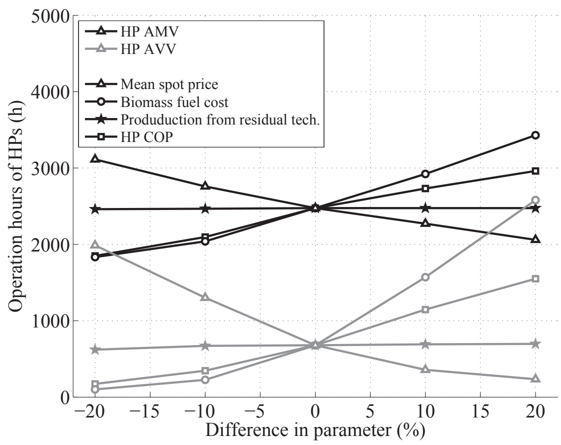


(d) Case #4 w/HP: Operation hours for the two HP units

Figure 10: Parametric analysis of the results from case #4 w/HP at forward temperatures of 70 °C

would require significant changes to the utilised models. On the other hand, the constraints of network capacities in distribution networks could be assessed individually, as transmission network flow profiles can be supplied as an input, based on the presented study.

## 5 Conclusion

The influence of DH network temperatures to the performance of utility production in Greater Copenhagen was investigated for forward temperatures between 40 to 110 °C. Two energy scenarios were considered, one current, which was validated model for 2011, and a future scenario, as proposed by energy planners for 2025, where reductions in carbon emissions for heat were of major interest. As neither of the two scenarios utilise central HPs for DH production, two additional scenarios were created to investigate if changed DH temperatures influenced the performance of this technology.

Compared to the current, the future scenario resulted in increased cost for consumers by approximately 15 %, but also carbon reductions above 50 % on both electricity and heat. The two scenarios showed similar trends for cost and emissions for reduced DH temperatures. Reduction in consumer cost were possible, with increasing magnitude with reductions in DH temperatures, until the point where electricity was needed to boost the temperatures of hot tap water in the individual dwellings.

Integration of central HPs became increasingly beneficial with reductions in DH temperatures. In a current scenario with central HPs installed, cost reductions of approximately 4-5 % were achieved, which further reduces carbon emissions from DH by more than 15 %. For future scenarios, cost reductions were further increased, but further reduction in carbon emissions for 2025 were barely possible with the considered HP technology. For both cases the maximal reduction of consumer cost was found for 60 °C forward temperature.

Based on the results, the authors recommend the use of 65-70 °C as the optimal forward temperature for DH networks, since lower temperatures require high investment, among others DH booster HP units in each dwelling. The difference between 60 and 70 °C forward temperatures corresponds to a difference of approximately 1.5-2 % on consumer costs for the future scenario.

The results were network specific, as they represent the specific generation technologies and demand curves and network capacities, but similar trends were found for the two different scenarios, and similar effects may thus also be expected for other large DH networks.

## Acknowledgement

This work was supported by Copenhagen Cleantech Cluster (CCC), DONG Energy and Danish Technological Institute (DTI)

## References

[1] Blarke, M.B.. Towards an intermittency-friendly energy system: Comparing electric boilers and heat pumps in distributed cogeneration. Applied Energy 2012;91(1):349–365.

[2] DONG Energy, . Annual report 2014 - Green, Independent and Cost-effective Energy. 2015. URL: http://assets.dongenergy.com/DONGEnergyDocuments/com/Investor/Annual_Report/2014/dong_energy_annual_report_en.pdf.

[3] Danish Government, . Government platform (in danish: Regeringsgrundlag). 2011. URL: http://www.stm.dk/publikationer/Et_Danmark_der_staar_sammen_11/Regeringsgrundlag_okt_2011.pdf; [accessed 25.03.14].

[4] City Council of Copenhagen, . CPH climate plan 2025 (in danish: KBH 2025 klimaplan - en grøn, smart og CO2-neutral by.). 2013. URL: http://cityclimateleadershipawards.com/copenhagen-cph-climate-plan-2025/; [accessed 25.03.14].

[5] CTR, HOFOR and VEKS, . Heat plan Greater Copenhagen 3 (in danish: Varmeplan Hovedstaden 3). 2014. URL: http://www.varmeplanhovedstaden.dk/publikationer-og-moeder; [accessed 25.03.14].

[6] Elmegaard, B., Houbak, N.. Simulaton of the Avedøreværket Unit 1 Cogeneration Plant with DNA. Proceedings of The 16th International Conference on Efficiency, Cost, Optimization, Simulation, and Environmental Impact of Energy Systems (ECOS 2003),; Technical University of Denmark; 2003,.

[7] Verbruggen, A.. Combined heat and power (CHP) essentials. International Journal of Energy Technology and Policy 2007;5(1):1–16.

[8] Lowe, R.. Combined heat and power considered as a virtual steam cycle heat pump. Energy Policy 2011;39(9):5528–5534.

[9] Ommen, T., Markussen, W.B., Elmegaard, B.. Heat pumps in combined heat and power systems. Energy 2014;76(0):989–1000.

[10] Ommen, T., Verda, V., Jensen, J.K., Markussen, W.B., Elmegaard, B.. Exergoeconomic optimisation of heat pumps in district heating systems. Energy 2015;xx(0):1–18. [submitted].
[11] SKAT, . Examples for calculation of taxreduction for various heat production units (in danish: Eksempler p beregning af afgiftslempelse for forskellige varmeproduktionsanlæg). 2014. URL: `https://skat.dk/SKAT.aspx?oID=2061615`; [accessed 05.12.14].
[12] Bach, B.. Integration of heat pumps in greater copenhagen. Master's thesis; Technical University of Denmark; 2014.
[13] Ommen, T.. Heat pumps in CHP systems - high-efficiency energy system utilising combined heat and power and heat pumps. Ph.D. thesis; Technical University of Denmark; 2015.
[14] CTR, HOFOR and VEKS, . Heat plan Greater Copenhagen 2 - options for CO2-neutral distict heating (in danish: Varmeplan Hovedstaden 2 - handlemuligheder for en CO2-neutral fjernvarme). 2014. URL: `http://www.varmeplanhovedstaden.dk/publikationer-og-moeder`; [accessed 25.03.14].
[15] F-Chart Software, . Engineering equation solver. 1992.
[16] Ferris, M.C.. Matlab and gams: Interfacing optimization and visualization software. Tech. Rep. 1; 2007.
[17] GAMS Development Corporation, . General algebraic modeling system. 1998. URL: `http://www.gams.com/`.
[18] IBM, . IBM ILOG CPLEX. 2009. URL: `www.ibm.com`.
[19] Centralkomunernes Transmissionsselskab I/S, . Technical key figures (in danish: Tekniske nøgletal). 2013. URL: `http://www.ctr.dk/teknik.aspx`; [accessed 02.02.15].
[20] Dansk Fjernvarme, . Benchmarking, statistics 2011/2012 (in danish: Benchmarking, statistik 2011/2012). 2013. URL: `http://www.fjernvarmen.dk/Faneblade/HentMaterialerFANE4/~/media/Publikationer/Aarsstatistikker/BenchmarkingStatistik20112012.ashx`; [accessed 26.09.13].
[21] Lund, H., Werner, S., Wiltshire, R., Svendsen, S., Thorsen, J.E., Hvelplund, F., et al. 4th generation district heating (4GDH). integrating smart thermal grids into future sustainable energy systems. Energy 2014;68:1–11.
[22] Zvingilaite, E., Ommen, T., Elmegaard, B., Franck, M.. Low Temperature District Heating Consumer Unit with Micro Heat Pump for Domestic Hot Water Preparation. District Energy Development Center; 2012, p. 136–143.
[23] Ommen, T.S., Elmegaard, B.. Exergetic evaluation of heat pump booster configurations in a low temperature district heating network. In: Desideri, U., Manfrida, G., Sciubba, E., editors. The 25th International Conference on Efficiency, Cost, Optimization and Simulation of Energy Conversion Systems and Processes (Perugia, June 26th-June 29th, 2012). Firenze University Press; 2012,.
[24] Elmegaard, B., Ommen, T.S., Markussen, M., Iversen, J.. Integration of space heating and hot water supply in low temperature district heating. Energy and Buildings 2015;:–doi:`http://dx.doi.org/10.1016/j.enbuild.2015.09.003`.
[25] Pirouti, M., Bagdanavicius, A., Ekanayake, J., Wu, J., Jenkins, N.. Energy consumption and economic analyses of a district heating network. Energy 2013;57:149–159. doi:`10.1016/j.energy.2013.01.065`.
[26] Dalla Rosa, A., Christensen, J.. Low-energy district heating in energy-efficient building areas. Energy 2011;36(12):6890–6899. doi:`10.1016/j.energy.2011.10.001`.
[27] Lin, F., Yi, J., Weixing, Y., Xuzhong, Q.. Influence of supply and return water temperatures on the energy consumption of a district cooling system. Applied Thermal Engineering 2001;21(4):511–521. doi:`10.1016/S1359-4311(00)00046-6`.
[28] Kvisgaard, B., Hadvig, S.. Varmetab fra fjernvarmeledninger : Heat loss from pipelines in district heating systems. Teknisk forlag; 1980. ISBN 8757106355, 9788757106350.
[29] Bøhm, B.. Simple methods for determination of heat losses from district heating pipes under normal conditions [in danish: Enkle metoder til bestemmelse af varmetab fra fjernvarmeledninger under normal drift]. Danmarks Tekniske Højskole, Lyngby (Denmark) and Sønderborg Fjernvarmeselskab A.m.b.A., Sønderborg (Denmark).; 1990. ISBN 8788038181, 9788788038187.
[30] Nord Pool Spot, . The power market. 2013. URL: `http://umm-archive.nordpoolspot.com/web/`; [accessed 02.02.15].
[31] Houbak, N.. Proposal for simulator contest. Proceedings of the 16th International ECOS conference. Volume 1, 2, and 3; DTU, Technical University of Denmark; 2003,.
[32] Berntsson, T.. Heat sources - technology, economy and environment. International Journal of Refrigeration 2002;25(4):428–438.
[33] Danish Standards, . Code of practise for domestic water supply installations (DS 439). 2009.
[34] Ommen, T., Markussen, W.B., Elmegaard, B.. Comparison of linear, mixed integer and non-linear programming methods in energy system dispatch modelling. Energy 2014;74:109–118.
[35] Nord Pool Spot, . UMM archive. 2013. URL: `http://www.nordpoolspot.com/How-does-it-work/`; [accessed 02.02.15].
[36] DONG Energy, . Environmental reports 2011. 2012. URL: `http://assets.dongenergy.com/DONGEnergyDocuments/com/Business%20Activities/Thermal%20Power/Environmental_Reports/2011/`; [accessed 23.03.14].
[37] Vattenfall A/S, . Environmental reports 2011 (in danish: Grønne regnskaber 2011). 2012. URL: `http://corporate.vattenfall.dk/globalassets/danmark/om_os/gronne_regnskaber/amagervaerket-gront-regnskab-2013.pdf`; [accessed 23.03.14].
[38] Energinet.dk, . Energinet.dk analytic prerequisites 2012-2035 [in danish: Energinet.dk's analyseforudsætninger 2012-2035]. Tech. Rep. 1; 2012.
[39] Energinet.dk, . Download of market data - elspot price, capacity on transmission lines etc. 2011. URL: `http://www.energinet.dk`.
[40] Danish Energy Agency, . Assumptions of socio- economic analysis in the energy sector [in danish: Forudsætninger for samfunds- økonomiske analyser påenergiområdet]. 2011. [accessed 10.10.13].
[41] Energinet.dk, . Guidelines for the environmental declaration of electricity [in danish: Retningslinjer for miljødeklarationen for el]. Tech. Rep. 1; 2015.
[42] EUDP - Energiteknologisk udvikling & demonstration, . Heat pumps for hot tap water in low tempera-

ture district heating networks. (in danish: Varmepumper til brugsvand i forbindelse med lavtemperaturfjernvarme). 2015. URL: http://www.energiteknologi.dk/da/project/varmepumper-til-brugsvand-i-forbindelse-med-lavtemperaturfjernvarme; [accessed 25.03.15].

[43] Verbruggen, A.. A systemmodel of combined heat and power generation in district heating. Resources and Energy 1982;4(3):231–263.

[44] Energinet.dk, . Introduction to system services (in danish: Introduktion til systemydelser, dok. 43532-13, sag 13/208). 2013. URL: http://www.energinet.dk.

[45] Energinet.dk, . Ancillary services to be delivered in denmark:tender conditions (in danish: Systemydelser til levering i danmark: Udbudsbetingelser). 2012. URL: http://www.energinet.dk.

[46] Amager Ressourcecenter, . Environmental reports (in danish: Miljøredegørelse). 2012. URL: http://www.a-r-c.dk/media/123663/miljoredegorelse_2012-pdf-.pdf; [accessed 23.03.14].

[47] Vestforbrænding, . Measurement and results (in danish: Måling og resultater). 2012. URL: http://www.vestfor.dk/web/10157/37@public; [accessed 23.03.14].

[48] KARA/NOVEREN I/S, . Environmental reports (in danish: Grønne regnskaber). 2012. URL: http://karanoveren.dk/karanoveren/organisation/groenne-regnskaber; [accessed 23.03.14].

**Nomenclature**

| | |
|---|---|
| $\dot{C}$ | cost rate, €/h |
| c | cost factor, €/MWh or € |
| $\dot{H}$ | flow rate of enthalpy, MWh/h |
| o | binary operation variable, - |
| $P$ | power, MW |
| $Q$ | quantity of heat in storage, MWh |
| $\dot{Q}$ | heat production, MJ/s |
| $r$ | ratio, - |
| UMM | availability input parameter, - |
| $v$ | binary design input parameter, - |
| **Greek symbols** | |
| $\beta$ | power loss factor by heat extraction, - |
| $\Delta$ | reduction, MJ/s |
| $\eta$ | efficiency, - |
| **Superscripts** | |
| 1 | below the "no-loss" point |
| 2 | above the "no-loss" point |
| elec | electric |
| ex. | extraction |
| max | maximum |
| min | minimum |
| rel | relative to maximum |

| | |
|---|---|
| **Subscripts** | |
| $f$ | other technologies |
| $g$ | heat pumps |
| $h$ | boilers |
| $i$ | CHP plants |
| $j$ | energy markets |
| $k$ | thermal unit sites |
| $l$ | transmission notes |
| $m$ | transmission networks |
| $n$ | distribution networks |
| $t$ | hours |
| **Abbreviations** | |
| CHP | Combined Heat and Power |
| COP | Coefficient of Performance |
| HP(s) | Heat Pump(s) |
| HS | Heat storage |
| O&M | operation and maintenance |
| TL | transmission losses |

# Appendices



## A Energy system model formulation

In this appendix, the key technical and economical constraints of the detailed system model are presented. As the economic constraints related to taxation are autonomous for each country, the reader is referred to [13] for further information on this specific topic for Danish conditions.
The model was implemented in General Algebraic Modelling System [17] using the mixed integer linear optimisation algorithm CPLEX [18]. External data processing is handled by Matlab, using the interface gdxmrw [16]. The implementation of energy system layout (eg. CHP-units, heat pumps or transmission capacity) is generic and easy to change from one case to another.

### A.1 Structure

The problem was considered over a period of time $\mathcal{T} = 1, \ldots, t$, which corresponds to the operation of the spot market. For each time periods, data for power plant load and the amount of stored heat at the termination of the period is passed on to the beginning of the subsequent period.
The heat and electricity demands, as well as the electricity produced at decentral CHP plants and by wind turbines in the region, were supplied as input to each of the time periods.
For the case where capital cost are considered as sunk cost, the objective function for minimisation of each time period was calculated as presented in Eq. 3 and further explained in section 2.5.
Several locations are used in the analysis. Traditional production areas for thermal units are indexed by $\mathcal{K}$. District heating transmission points (collection of streams) are indexed by $\mathcal{L}$. Transmission networks are indexed by $\mathcal{M}$ and the distribution networks by $\mathcal{N}$.

### A.2 Economic constraints

For most of the assessed technologies, the cost of utility production at an individual unit depends on the unit type, its efficiency, operation and maintenance cost and the type of fuel. Apart from direct fuel cost, the individual fuel types may further be affected by different taxation or subsidy schemes or by additional transportation and handling cost. The operation and maintenance cost included in the model correspond to the variable contribution.
In the following sections, the economic constraints are listed for individual unit types. Note that the description of power plants represents several types: extraction CHP, back pressure CHP and condensing power plants.

#### A.2.1 Power plants

The total cost rate of production at the individual plant was calculated based on various components. The method for calculation of the individual components was similar for most of the contributions. The total cost rate was calculated according to eq. A.1.

$$\dot{C}_{i,t}^{\mathrm{CHP}} = \dot{C}_{i,t}^{\mathrm{fuel}} + \dot{C}_{i,t}^{\mathrm{taxes}} - \dot{C}_{i,t}^{\mathrm{subsidy}} + \dot{C}_{i,t}^{\mathrm{VAT}} + \dot{C}_{i,t}^{\mathrm{startup/shutdown}} \qquad , i \in \mathcal{I}, t \in \mathcal{T}. \tag{A.1}$$

The individual components of the total cost rate are dependent on the consumption of fuel and/or the production of electricity and heat. All of the individual contributions to the total cost rate for CHP units are required to be positive. In the case of fuel cost $\dot{C}_{i,t}^{\mathrm{fuel}}$ the contributions are included in eq. A.2.

$$\dot{C}_{i,t}^{\mathrm{fuel}} = c_i^{\mathrm{fuel}} \cdot \dot{H}_{i,t} + c_i^{\mathrm{O\&M}} \cdot P_{i,t} \qquad , i \in \mathcal{I}, t \in \mathcal{T}. \tag{A.2}$$

where $\dot{H}$ is the flow rate of enthalpy for combustion, and $P$ is the produced electricity. The individual fuel cost factor $c_i^{\mathrm{fuel}}$ for the plants were calculated based on fuel type and transportation and handling cost [40].
The cost factor for operation and maintenance $c_i^{\mathrm{fuel}}$ corresponds to the variable cost for utility production.
A similar approach has been used to calculate the contribution from subsidised fuels $\dot{C}_{i,t}^{\mathrm{subsidy}}$.
The cost rates for startup and shutdown were calculated as presented in eq. A.3.

$$\begin{aligned}\dot{C}_{i,t}^{\mathrm{startup/shutdown}} &= c_i^{\mathrm{startup}} \cdot o_{i,t}^{\mathrm{startup}} + c_i^{\mathrm{shutdown}} \cdot o_{i,t}^{\mathrm{shutdown}} \\ &\quad , o_{i,t}^{\mathrm{startup}}, o_{i,t}^{\mathrm{shutdown}} \in \{0,1\}, i \in \mathcal{I}, t \in \mathcal{T}.\end{aligned} \tag{A.3}$$

The cost $c_i^{\mathrm{startup}}$ and $c_i^{\mathrm{shutdown}}$ represent the variable cost of changing the operation between on and off. The binary variables $o_{i,t}^{\mathrm{startup}}$ and $o_{i,t}^{\mathrm{shutdown}}$ are controlled by the optimisation algorithm, and further described in section A.4.

#### A.2.2 Heat boilers

The employed method for calculation of the heat boilers was similar to the approach utilised for section A.2.1. The calculation of the total cost rate is presented in eq. A.4.

$$\dot{C}^{\text{boiler}}_{h,t} = \dot{C}^{\text{fuel}}_{h,t} + \dot{C}^{\text{taxes}}_{h,t} + \dot{C}^{\text{VAT}}_{h,t} \qquad , h \in \mathcal{H}, t \in \mathcal{T}. \tag{A.4}$$

All of the individual contributions to the total cost rate for boilers are required to be positive. The fuel cost was calculated based on fuel consumption and the production-dependent element of the operation and maintenance cost, which corresponds to the produced heat.

$$\dot{C}^{\text{fuel}}_{h,t} = c^{\text{fuel}}_{h} \cdot \dot{H}_{h,t} + c^{\text{O\&M}}_{h} \cdot \dot{Q}_{h,t} \qquad , h \in \mathcal{H}, t \in \mathcal{T}. \tag{A.5}$$

A similar approach was used to calculate the cost rates for the remaining elements of eq. A.4.

#### A.2.3 Electricity-driven heat pumps

In the case of electricity-driven heat pumps, the total cost rate does not include the cost of consumed electricity, as the electricity is covered by other elements of the objective function eq. 3 and by the energy balances in section A.3. The remaining elements are presented in Eq. A.6.

$$\dot{C}^{\text{HP}}_{g,t} = \dot{C}^{\text{O\&M}}_{g,t} + \dot{C}^{\text{taxes}}_{g,t} + \dot{C}^{\text{VAT}}_{g,t} \qquad , g \in \mathcal{G}, t \in \mathcal{T}. \tag{A.6}$$

All of the individual contributions to the total cost rate for HP units are required to be positive. The contribution from O&M corresponds to the variable expenses of operating a heat pump. For the case where the heat pump uses electricity supplied from the distribution grid, a network tariff is used, in order to take the distribution losses of such networks into account.

$$\dot{C}^{\text{O\&M}}_{g,t} = c^{\text{O\&M}}_{g} \cdot \dot{Q}_{g,t} + c^{\text{networktariff}}_{g} \cdot P_{g,t} \qquad , g \in \mathcal{G}, t \in \mathcal{T}. \tag{A.7}$$

### A.3 Electricity and heat balances

In modern energy systems, significant effort is put on balancing of the production and demand at correct location and time. The electricity transmission grid within the bidding area was modelled as one uniform network without bottlenecks for either of the utility units or consumers.

The electricity demand $P^{\text{consumer}}_{t}$ including distribution losses was used for the analysis in the electricity balance eq. A.8.

$$P^{\text{transmission}}_{t} - \sum_{g \in \mathcal{G}} P_{g,t} - \sum_{j \in \mathcal{J}} P^{\text{export}}_{j,t} = P^{\text{consumer}}_{t} \qquad , t \in \mathcal{T}. \tag{A.8}$$

where $P^{\text{transmission}}_{t}$ is the flow of electricity from the transmission network, $P_{g,t}$ is the consumed electricity from a specific heat pump, and $P^{\text{export}}_{j,t}$ is the export of electricity to a specific area.

The transmission is supplied by thermal units, other units such as wind turbines and decentral CHP units, and import of electricity.

$$\sum_{i \in \mathcal{I}} P_{i,t} + \sum_{f \in \mathcal{F}} P^{\text{other}}_{f,t} + \sum_{j \in \mathcal{J}} P^{\text{import}}_{j,t} = P^{\text{transmission}}_{t} / (1 - \eta_{\text{TL}}) \qquad , t \in \mathcal{T}. \tag{A.9}$$

In this way all electricity flows into the network are subject to losses. The magnitude of transmission losses ($\eta_{\text{TL}}$) was determined based on historical data following a similar procedure. Both import and export of electricity are further constrained by the interconnection capacity of the two bidding areas. All of the variables in eq. A.8 and A.9 are required to be positive.

The heat balances used in the analysis followed a similar setup. The transmission network for heat is split into several areas, with detailed knowledge of the transmission capacity between each area. Opposite to the electricity demand, the heat demand is split into appropriate locations, according to the detailed data from the transmission operators. For all of the considered areas, energy balances ensure logic distribution and prevent accumulation in areas without storage options.

Two examples of heat balances are presented for introduction of units in transmission and distribution networks in eq. A.10 and eq. A.11.

$$\sum_{i\in\mathcal{I}} \dot{Q}_{i,k,t} + \sum_{h\in\mathcal{H}} \dot{Q}_{h,k,t} + \sum_{g\in\mathcal{G}} \dot{Q}_{g,k,t} = \sum_{l\in\mathcal{L}} \dot{Q}_{l,k,t} \qquad , k \in \mathcal{K}, t \in \mathcal{T}. \tag{A.10}$$

where $\dot{Q}_{l,k,t}$ is the transferred heat from production area $k$ to the transmission point $l$. An example of the capacity limitations of the transmission network is addressed in eq. A.12. In the heat distribution network, heat is transferred from a transmission area $m$ to the distribution network $n$ using the variable $\dot{Q}_{n,m,t}$.

$$\sum_{m\in\mathcal{M}} \dot{Q}_{n,m,t} + \sum_{o\in\mathcal{O}} \dot{Q}_{o,n,t} + \sum_{p\in\mathcal{P}} \dot{Q}_{p,n,t} = \dot{Q}_{n,t} \qquad , n \in \mathcal{N}, t \in \mathcal{T}. \tag{A.11}$$

where $\dot{Q}_{n,t}$ is the demand for heat in area $n$ at time $t$. All of the variables in eq. A.10 and A.11 are required to be positive.

The limitations in transmission capacity, as well as in other connections of the DH network, is introduced as presented in eq. A.12.

$$\sum_{l\in\mathcal{L}} \dot{Q}_{l,k,t} \leq \dot{Q}^{\max}_{l,k} \qquad , k \in \mathcal{K}, t \in \mathcal{T}. \tag{A.12}$$

where $\dot{Q}^{\max}_{l,k}$ is the maximal allowed transmission capacity in (MJ/$s$)

### *A.3.1 Heat storages*

Heat storages may be located at any position in the network, but according to the actual locations in the energy system case, the storages was only introduced in the transmission networks. Besides the integration in the network, five equations govern the operation of the storage. The overall heat balance for the unit is presented in eq. A.13.

$$Q_{m,t} + Q^{\text{in}}_{m,t} - Q^{\text{out}}_{m,t} - Q^{\text{heatloss}}_{m,t} = Q_{m,t+1} \qquad , m \in \mathcal{M}, t \in \mathcal{T}. \tag{A.13}$$

where $Q_{m,t}$ denotes the heat available in the storage at time $t$, and $Q_{m,t+1}$ in the subsequent time step. All five elements are required to be positive in the optimisation. The heat losses related to heat storage was calculated according to eq. A.14. Low heat losses for short time heat storage are expected due to mixing of stratified layers and temperature differences to the ambient.

$$Q^{out}_{m,t} \cdot (1 - \eta_{\text{HS}}) = Q^{\text{heatloss}}_{m,t} \qquad , m \in \mathcal{M}, t \in \mathcal{T}. \tag{A.14}$$

Three additional constraints were set to represent the physical dimensions and design of the heat storage. The constraints are presented in eq. A.15 to A.17. Eq. A.15 describes the installed capacity, where $Q^{\text{max,size}}_{m,t}$ is the maximal allowed stored heat in (MWh). Eq. A.16 and A.17 limit the charge and discharge of the storage, where $Q^{\text{max,rate}}_{m,t}$ is the maximal allowed rate per hour.

$$Q_{m,t} \leq Q_{m,t}^{\text{max,size}} \quad , m \in \mathcal{M}, t \in \mathcal{T}. \tag{A.15}$$

$$Q_{m,t}^{\text{in}} \leq Q_{m,t}^{\text{max,rate}} \quad , m \in \mathcal{M}, t \in \mathcal{T}. \tag{A.16}$$

$$Q_{m,t}^{\text{out}} \leq Q_{m,t}^{\text{max,rate}} \quad , m \in \mathcal{M}, t \in \mathcal{T}. \tag{A.17}$$

### *A.4 Technology constraints*

The considered technologies are common utility units which are utilised in many large district heating networks. A large fraction of the utilized technology constraints are presented for each of the individual technologies.

In the following sections, the constraints are listed for the individual unit types.

#### *A.4.1 Power plants*

The technical constraints for the power plants were defined in order to represent several types. In this way it is possible to include extraction CHP, back pressure CHP and condensing power plants using few equations. The maximum and minimum technical load in terms of fuel consumption for a power plant unit was described according to Eq A.18 and Eq. A.19. The operation of the unit is dependent on a binary operation variable $o_{i,t}$ and its availability $\text{UMM}_{i,t}$ according to availability data (historical data for validation).

For the specific fuel load, the electricity production in full back pressure was calculated according to Eq. A.21. A reduction in electric efficiency was modelled assuming a constant contribution at full load. The trend of the derived model is presented in Fig. A.1. The high reduction scheme fits well with the results of the AVV1 model within the typical load range.

A constant boiler efficiency was assumed for the full range of applicable loads. The heat production in back pressure operation was evaluated as the residual of the total utilisation of fuel and the back pressure electricity production according to Eq. A.22, where the thermal efficiency $\eta_i^{total}$ corresponds to the lower heating value of the utilised fuel.

The produced electricity of the unit was calculated according to Eq. A.23. A reduction in heat production of an extraction CHP plant ($\Delta\dot{Q}_{i,k,t}^1 + \Delta\dot{Q}_{i,k,t}^2$) leads to increased power production according to power loss factors by heat extraction $\beta^1$,$\beta^2$ [-] [43]. $\beta^1$ corresponds to heat extraction below the "no-loss" point, $\beta^2$ for heat extraction above this operational limit. The binary input parameter $v_i^{\text{ex.}}$ is used to distinguish between units with extraction points and units with only one production scheme (e.g. electricity only or back pressure units). Some of the investigated back pressure units allow the operator to bypass the turbine, in order to utilise the steam for boosting the heat production. The binary input parameter $v_i^{\text{bypass}}$ is used to distinguish such units from the remaining. The reduction in electricity from bypassing the turbine is denoted $P_{i,k,t}^{\text{bypass}}$.

By use of eq A.24 and A.25 it was ensured that the change from one power loss factor to the other corresponds to the physical requirement of the extraction CHP plant. If the binary variable $o_{i,t}^{\text{no}-\text{loss}}$ is 1, $\beta^2$ should be used, otherwise $\beta^1$. The no-loss point was located as the ratio $r_i^{\text{no}-\text{loss}}$ between heat extracted above and below the no loss point. The binary variable $o_{i,t}^{\text{no-loss}}$ was further used in Eq. A.26 and A.27 to determine the heat extraction.

The resulting heat from the extraction plant is determined by the Eq. A.28 to A.30. Eq. A.31 ensures that steam bypass corresponds to the bypassed amount of electricity.

For the case where power plants are constrained by rapid ramping of the boiler load, the model includes constraints designed to describe this operation restriction. The constraints were modelled as a limiting difference in load $\dot{H}_{i,k,t}^{\text{rel}}$ of the boiler from one hour to the next. As in Eq. A.32 and A.33 the constraints for startup and shutdown were included in these constraints, and correspond to the additional cost described in A.3. The constraints of Eq. A.34 and A.35 ensure that startup and shutdown only occurs in case of changed production commitment.

Technical and operational power plant constraints:

$$
\begin{aligned}
\dot{H}^{\max}_{i,k} \cdot o_{i,t} \cdot \mathrm{UMM}_{i,t} \geq & \dot{H}_{i,k,t} && , o_{i,t} \in \{0,1\}, i \in \mathcal{I}, k \in \mathcal{K}, t \in \mathcal{T}. && \text{(A.18)}\\
\dot{H}^{\min}_{i,k} \cdot o_{i,t} \leq & \dot{H}_{i,k,t} && , o_{i,t} \in \{0,1\}, i \in \mathcal{I}, k \in \mathcal{K}, t \in \mathcal{T}. && \text{(A.19)}\\
\eta^{\text{backp.}}_{i} = & \eta^{\text{elec}}_{i} + \eta^{\text{reduc.}}_{i} && , i \in \mathcal{I}. && \text{(A.20)}\\
P^{\text{backp.}}_{i,k,t} = & \dot{H}_{i,k,t} \cdot \eta^{\text{backp.}}_{i} - \dot{H}^{\max}_{i,k} \cdot \eta^{\text{reduc.}}_{i} \cdot o_{i,t} && , o_{i,t} \in \{0,1\}, i \in \mathcal{I}, k \in \mathcal{K}, t \in \mathcal{T}. && \text{(A.21)}\\
\dot{Q}^{\text{backp.}}_{i,k,t} = & \dot{H}_{i,k,t} \cdot \eta^{\text{total}}_{i} - P^{\text{backp.}}_{i,k,t} && , i \in \mathcal{I}, k \in \mathcal{K}, t \in \mathcal{T}. && \text{(A.22)}\\
P_{i,k,t} = & P^{\text{backp.}}_{i,k,t} + \beta^{1}_{i} \cdot \Delta\dot{Q}^{1}_{i,k,t} \cdot v^{\text{ex.}}_{i} + \beta^{2}_{i} \cdot \Delta\dot{Q}^{2}_{i,k,t} \cdot v^{\text{ex.}}_{i} && &&\\
& - P^{\text{bypass}}_{i,k,t} \cdot v^{\text{bypass}}_{i} && , i \in \mathcal{I}, k \in \mathcal{K}, t \in \mathcal{T}. && \text{(A.23)}
\end{aligned}
$$

$$
\begin{aligned}
\Delta\dot{Q}^{1}_{i,k,t} - \dot{H}^{\max}_{i,k} \cdot o^{\text{no-loss}}_{i,t} \leq & \dot{H}^{\max}_{i,k} \cdot r^{\text{no-loss}}_{i} \cdot (\eta^{\text{total}}_{i} - \eta^{\text{elec}}_{i}) \cdot v^{\text{ex.}}_{i} && , o^{\text{no-loss}}_{i,t} \in \{0.1\}, i \in \mathcal{I}, k \in \mathcal{K}, t \in \mathcal{T}. && \text{(A.24)}\\
\Delta\dot{Q}^{1}_{i,k,t} + \dot{H}^{\max}_{i,k} \cdot (1 - o^{\text{no-loss}}_{i,t}) \geq & \dot{H}^{\max}_{i,k} \cdot r^{\text{no-loss}}_{i} \cdot (\eta^{\text{total}}_{i} - \eta^{\text{elec}}_{i}) \cdot v^{\text{ex.}}_{i} && , o^{\text{no-loss}}_{i,t} \in \{0.1\}, i \in \mathcal{I}, k \in \mathcal{K}, t \in \mathcal{T}. && \text{(A.25)}\\
\Delta\dot{Q}^{1}_{i,k,t} \leq & \dot{H}^{\max}_{i,k} \cdot r^{\text{no-loss}}_{i} \cdot (\eta^{\text{total}}_{i} - \eta^{\text{elec}}_{i}) \cdot v^{\text{ex.}}_{i} && , i \in \mathcal{I}, k \in \mathcal{K}, t \in \mathcal{T}. && \text{(A.26)}\\
\Delta\dot{Q}^{2}_{i,k,t} \leq & \dot{H}^{\max}_{i,k} \cdot (1 - r^{\text{no-loss}}_{i}) && &&\\
& \cdot (\eta^{\text{total}}_{i} - \eta^{\text{elec}}_{i}) \cdot o^{\text{no-loss}}_{i,t} \cdot v^{\text{ex.}}_{i} && , o^{\text{no-loss}}_{i,t} \in \{0.1\}, i \in \mathcal{I}, k \in \mathcal{K}, t \in \mathcal{T}. && \text{(A.27)}
\end{aligned}
$$

$$
\begin{aligned}
\dot{Q}^{\text{backp.}}_{i,k,t} - \dot{Q}^{1}_{i,k,t} = & \Delta\dot{Q}^{1}_{i,k,t} \cdot v^{\text{ex.}}_{i} && , i \in \mathcal{I}, k \in \mathcal{K}, t \in \mathcal{T}. && \text{(A.28)}\\
\dot{Q}^{1}_{i,k,t} - \dot{Q}^{2}_{i,k,t} = & \Delta\dot{Q}^{2}_{i,k,t} \cdot v^{\text{ex.}}_{i} && , i \in \mathcal{I}, k \in \mathcal{K}, t \in \mathcal{T}. && \text{(A.29)}\\
\dot{Q}_{i,k,t} = & \dot{Q}^{2}_{i,k,t} + \dot{Q}^{\text{bypass}}_{i,k,t} \cdot v^{\text{bypass}}_{i} && , i \in \mathcal{I}, k \in \mathcal{K}, t \in \mathcal{T}. && \text{(A.30)}\\
\dot{Q}^{\text{bypass}}_{i,k,t} = & P^{\text{bypass}}_{i,k,t} \cdot v^{\text{bypass}}_{i} && , i \in \mathcal{I}, k \in \mathcal{K}, t \in \mathcal{T}. && \text{(A.31)}
\end{aligned}
$$

$$
\begin{aligned}
0 \leq & \dot{Q}_{i,k,t}, \dot{Q}^{1}_{i,k,t}, \dot{Q}^{2}_{i,k,t}, \dot{Q}^{\text{bypass}}_{i,k,t}, \dot{Q}^{\text{backp.}}_{i,k,t}, \Delta\dot{Q}^{1}_{i,k,t}, \Delta\dot{Q}^{2}_{i,k,t}\\
0 \leq & P_{i,k,t}, P^{\text{bypass}}_{i,k,t}, P^{\text{backp.}}_{i,k,t}, \dot{H}_{i,k,t}
\end{aligned}
$$

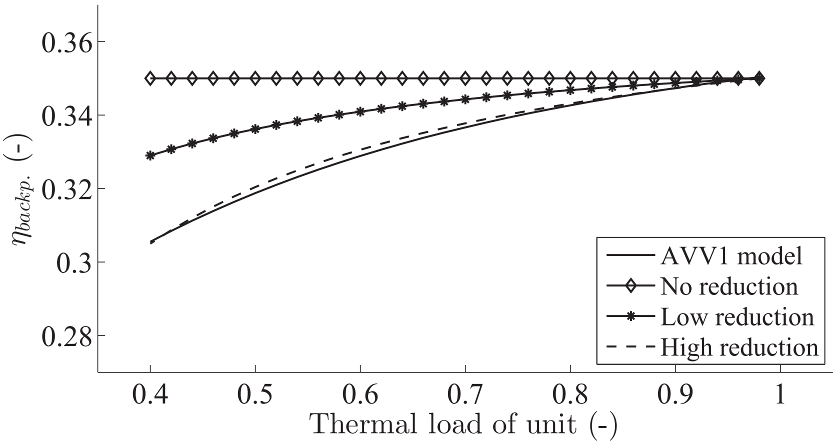


Figure A.1: Estimated reduction of electric efficiency at low unit loads

$$\begin{aligned}
\dot{H}^{\text{rel}}_{i,k,t+1} - \dot{H}^{\text{rel}}_{i,k,t} \leq & \dot{H}^{\text{rel,max}}_{i,k} \cdot (1 - o^{\text{startup}}_{i,t+1}) + \dot{H}^{\text{rel,startup}}_{i,k} \cdot o^{\text{startup}}_{i,t+1} \\
& , o^{\text{startup}}_{i,t} \in \{0,1\}, i \in \mathcal{I}, k \in \mathcal{K}, t \in \mathcal{T}. && \text{(A.32)} \\
\dot{H}^{\text{rel}}_{i,k,t} - \dot{H}^{\text{rel}}_{i,k,t+1} \leq & \dot{H}^{\text{rel,max}}_{i,k} \cdot (1 - o^{\text{shutdown}}_{i,t+1}) + \dot{H}^{\text{rel,shutdown}}_{i,k} \cdot o^{\text{shutdown}}_{i,t+1} \\
& , o^{\text{shutdown}}_{i,t} \in \{0,1\}, i \in \mathcal{I}, k \in \mathcal{K}, t \in \mathcal{T}. && \text{(A.33)} \\
o^{\text{startup}}_{i,t} \geq & o^{\text{CHP}}_{i,t} - o^{\text{CHP}}_{i,t-1} \\
& , o^{\text{CHP}}_{i,t}, o^{\text{startup}}_{i,t} \in \{0,1\}, i \in \mathcal{I}, t \in \mathcal{T}. && \text{(A.34)} \\
o^{\text{shutdown}}_{i,t} \geq & o^{\text{CHP}}_{i,t} - o^{\text{CHP}}_{i,t+1} \\
& , o^{\text{CHP}}_{i,t}, o^{\text{shutdown}}_{i,t} \in \{0,1\}, i \in \mathcal{I}, t \in \mathcal{T}. && \text{(A.35)}
\end{aligned}$$

### *A.4.2 Heat boilers*

Two sets of heat boiler constraints were included in the model, one for each location type (central vs. decentral). In this section the constraints of the central installations are presented. The maximum technical load in terms of fuel consumption for a boiler unit was described according to Eq A.36.
The resulting heat production was described according to Eq. A.37, where the thermal efficiency $\eta^{\text{total}}_h$ corresponds to the lower heating value of the utilised fuel.

$$\begin{aligned}
\dot{H}^{\max}_{h,k} \geq & \dot{H}_{h,k,t} && , h \in \mathcal{H}, k \in \mathcal{K}, t \in \mathcal{T}. && \text{(A.36)} \\
\dot{Q}_{h,k,t} = & \dot{H}_{h,k,t} \cdot \eta^{\text{total}}_h && , h \in \mathcal{H}, k \in \mathcal{K}, t \in \mathcal{T} && \text{(A.37)}
\end{aligned}$$

### *A.4.3 Heat pumps*

Two sets of heat pump constraints were included in the model, one for each location type (central vs. decentral). In this section the constraints of the central installations are presented. The produced heat of the unit was calculated using a coefficient of performance, and the consumed electricity, as presented in Eq. A.38.
For certain types of installations, operation of the heat pump unit will depend on external factors, such as operation at a specific power plant or facility. For other types, the unit capacity and COP may vary according to ambient temperatures or heat source flow rates. In order to address such cases, the coefficient of performance $COP_{g,t}$ and the capacity constraint $\dot{Q}^{\max}_{g,k,t}$ of the heat pump units were split at hourly basis,

and a binary operation variable $o^{\mathrm{HP}}_{g,t}$ was introduced. The capacity of such systems were calculated according to Eq. A.39.

$$\dot{Q}_{g,k,t} = COP_{g,t} \cdot P_{g,k,t} \qquad , g \in \mathcal{G}, k \in \mathcal{K}, t \in \mathcal{T}. \tag{A.38}$$

$$\dot{Q}^{\max}_{g,k,t} \cdot o^{\mathrm{HP}}_{g,t} \geq COP_{g,t} \cdot P_{g,k,t} \qquad , o^{\mathrm{HP}}_{g,t} \in \{0,1\}, g \in \mathcal{G}, k \in \mathcal{K}, t \in \mathcal{T} \tag{A.39}$$

*A.5 System reserves and operational constraints*

In order for the model to correspond to the operation of a specific energy system, additional constraints are needed to fully describe for cooperation of units and the different types of system reserves required. Many of the constraints are specified in publications from the system operator [44] [45]. For both manual and frequency reserve capacity the available reserve from a power plant unit was calculated according to Eq. A.40 and A.41 for the individual units. The individual reserve types were further constrained by minimum and maximum constributions from each unit.

$$\begin{aligned} P^{\mathrm{reserve}}_{i,t} \leq & \sum_{k \in \mathcal{K}} (\dot{H}_{i,k}) \cdot o_{i,t} \cdot \eta^{\mathrm{elec}}_i \cdot \dot{H}^{\mathrm{rel,reserve}}_i \\ & + \sum_{k \in \mathcal{K}} (\dot{H}_{i,k}) \cdot o_{i,t} \cdot (\eta^{\mathrm{total}}_i - \eta^{\mathrm{elec}}_i) \cdot \dot{H}^{\mathrm{rel,reserve}}_i \cdot (\beta^1_i + \beta^2_i)/2 \\ & , o_{i,t} \in \{0,1\}, i \in \mathcal{I}, t \in \mathcal{T}. \end{aligned} \tag{A.40}$$

$$\begin{aligned} P^{\mathrm{reserve}}_{i,t} \leq & \sum_{k \in \mathcal{K}} (\dot{H}_{i,k}) \cdot o_{i,t} \cdot UMM_i \cdot \eta^{\mathrm{elec}}_i \cdot \dot{H}^{\mathrm{rel,reserve}}_i \\ & + \sum_{k \in \mathcal{K}} (\Delta \dot{Q}^1_{i,k,t}) \cdot \beta^1_i + \sum_{k \in \mathcal{K}} (\Delta \dot{Q}^2_{i,k,t}) \cdot \beta^2_i - \sum_{k \in \mathcal{K}} (P_{i,k,t}) \\ & , o_{i,t} \in \{0,1\}, i \in \mathcal{I}, t \in \mathcal{T}. \end{aligned} \tag{A.41}$$

The sum of the individual reserves were required to exceed a predefined value for both types of reserves. Additional operational constraints exist, e.g. considerations for operating the steam network, as well as multifuel units with mutual steam turbines and/or gas turbines.
Ensuring short-circuit power, reactive reserves and voltage control was addressed by ensuring 3 large power plants ( $P \geq 150$ MW) to be committed at all time.

## B Energy system model validation

The system model has been validated against a number of data series from various sources with different time resolutions. The comparison with one of the data sources is presented in this appendix. Further results of the validation may be found in [13].
A number of assumptions are used for performance of the individual plants, heat network capacities and fuel costs. Historical data are used where available. Both technology and cost data are presented in Table 8a. Such data are considered constant throughout the year, although the efficiency of many units will vary according to DH temperatures.
By examination of the accuracy and detail of representative segments, it is shown that the model presents good agreement with the historical data. Thus the model is considered applicable to investigate the interaction between several production technologies in a system where both heat and electricity costs are optimized for each hour.

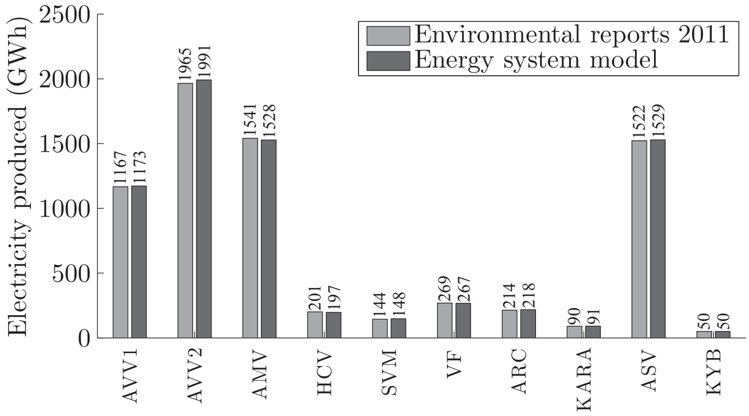


(a) Electricity

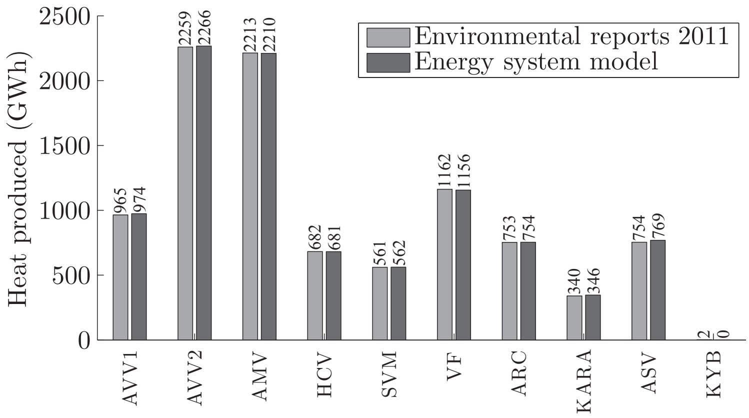


(b) Heat

Figure B.2: Comparison of produced electricity according to environmental reports 2011 and the model. Results correspond to entire power stations, except for AVV1 and AVV2 units.

### *B.1 Environmental reports*

Based on data for environmental reports for 2011 from the companies [36, 37] and municipal cooperatives [46, 47, 48] operating the considered thermal power plant, it is possible to compare the real production of the actual units, with the calculated production, for a given year (2011). The two comparisons are presented in Fig. B.2a and B.2b for electricity and heat, respectively.

For most of the considered power plants, data is available for the entire power station, which may represent between 1 (eg. KARA) and 5 (Kyndby power station - KYB) units. For Avedøre power station, the data is available for unit 1 and unit 2 individually, where unit 2 represents a steam turbine with two boilers and two gas turbines in cooperation. The presented data series show close matches for both electricity and heat for the individual power plants.

In the case of KYB (peak load and backup unit), a very small separate district heating network exists, which was not included in the model. For the remaining power stations the difference between actual and modelled production is between 0-2 %, except for SVM where deviation of electricity production is approximately 3 % which in absolute value is only approximately 4 GWh. For ASV the considered heat demand of Kalundborg (Asnæs) and the corresponding data from the environmental report differs approximately 2 % or 16 GWh.

All together, the considered power plants produce a marginally higher amount of electricity and heat in the model compared to the operation data from 2011. This corresponds to approximately 31 GWh electricity and 29 GWh heat.